Final Research Performance Progress Report
Reporting Period: 10/01/2017-3/31/2022
Date of Submission of Report: April 07, 2022

Federal Agency/ Organization Element:	DOE/EERE/ Vehicle Technologies Office (VTO)
FOA Name and Number:	DE-FOA-0001629
Award Number:	DE-EE0008231
Award Type:	Cooperative Agreement
Project Title:	Solvent-Free and Non-Sintered 500 Wh/kg All Solid-State Battery
Budget Period **Project Period:**	10/01/2017 – 3/31/2022 10/01/2017 – 3/31/2022
Recipient Organization:	Navitas Advance Solutions Group, LLC
Recipient Type:	Private company
DUNS Number:	07-8782-193
Principal Investigator	James Dong, Ph.D. Research Director, (734)-205-1408, jdong@navitassys.com
Business Contact:	Ben Benedict
Partners:	University of Maryland, Oak Ridge National Lab
DOE Technology Manager:	Tien Duong, DOE Technology Manager, tien.duong@ee.doe.gov
DOE Project Officer:	Adrienne Riggi, DOE Technical Project Officer, adrienne.riggi@netl.doe.gov
Submitting Official:	Ben Benedict, Office Administrator, (734)-205-1410, bbenedict@navitassys.com

Collaborations. This project funds work at Navitas, UMD, and ORNL. Contributors involved: **Navitas:** Dr. James Dong, Dr. Michael Wixom, Dr. Kuber Mishra, Dr. Tianhong Xu, Mahdi Soueid, Laura Bass, Kahla Sardo, Brendan Skelly. **UMD:** Dr. Chunsheng Wang, Xinzi He. **ORNL:** Dr. Zhijia Du.

EXECUTIVE SUMMARY

Navitas Advanced Solutions Group (Navitas) will lead a team including University of Maryland (UMD) and Oak Ridge National Laboratory (ORNL) to demonstrate a solvent-free (dry) process enabling the fabrication of all-solid Li batteries. This project will address technical and economic challenges associated with processing of solid ion conductors and integrating them into large format batteries for energy storage. The solid-state electrolyte (SSE) material will be a doped sulfide with high Li ion conductivity and chemical stability. A cathode-separator bilayer will be fabricated through a solvent-free roll mill operation, followed by a single-step lamination to assemble a multi-layer stack. This innovative approach circumvents the mechanical limitations of handling a free-standing SSE, the processing limitations of vapor deposition, and the thermal expansion incompatibilities associated with sintering. If successful, the outcome of this project will be a solid-state battery pairing high nickel NMC cathode and protected lithium metal anode.

The proposed technology will address key limitations of state-of-the-art lithium batteries to meet DOE EV battery targets and accelerate their adoption as large format electric vehicle batteries for sustainable transportation technology. Based on scalable processing and acceptable bill of material costs, the proposed innovation will reduce cell costs below $100/kWh and address the key barrier to electric vehicle adoption. This approach will support the Battery 500 Program in demonstrating a fabrication method capable of producing a cell with specific energy of ≥ 500 Wh/kg able to achieve 1000 cycles.

Innovative Approach

To accomplish these goals, Navitas was teaming with UMD and ORNL to establish a reliable scientific research team. Navitas will address processing limitations of state-of-the-art solid electrolytes by extending solvent-free electrode fabrication technology to the scalable production of cathode/solid electrolyte laminates. Limited conductivity dictates that solid electrolytes be thin films.

Solvent-free roll-to-roll electrode production technology that has been commercialized by Maxwell Technologies for ultracapacitors and modified by Navitas and others for LIBs. This represents an innovative approach to address the scalability and mechanical limitations of established solid-state electrolytes to maintain. Roll-to-roll processing in a production environment will drive down the high $/Wh for today's thin film solid state batteries. Combined with the vastly enhanced abuse tolerance, system level cost below 0.1 $/Wh are attainable through simplifying controls and reducing thermal management components. This overall impact will be scalable production of large format all solid batteries required by the vehicle and stationary markets.

The Navitas team’s innovation starts with a solid-state sulfide electrolyte able to meet the keystone conductivity challenge in a film of practical thickness (20 - 50 µm). The electrolyte will be based on a composite of PTFE, carbon, and stabilized sulfide. This formulation builds on extensive recent development by Navitas of a solvent-free process to fabricate LIB electrodes.

Navitas developed new formulations to include conductive additives and processing aids. Navitas optimized the active material content in the electrode, reducing binder content by over 50%. Taking a similar approach, Navitas expects to be able to produce a sulfide film that attains 50% of its intrinsic bulk ionic conductivity and is flexible and mechanically robust to downstream operations in high volume cell assembly.

The polymer/inorganic composite approach by the Navitas team will enable an innovative extrusion/lamination of a continuous and flexible cathode/electrolyte film. Electrolyte film on the cathode will be a free-standing component or film. An air-stable (> 8 hours in dry room) sulfide electrolyte will be developed at UMD. The solid electrolyte will have a wide electrochemical stability (0-5V). The area and thickness of the solid electrolyte can be > 50 cm^2 and < 20 µm. With optimization, the ionic conductivity is expected to reach 10^{-3} S/cm. The solid electrolyte would allow long term cycling (> 500 cycles) of Li/SSE/Li cell at > 3 mA/cm^2 with the utilization of Li > 80%. The energy-efficient and high-throughput process will reduce cost of the solid electrolyte (< $\$10/m^2$).

SECTION I. ACCOMPLISHMENTS & ACTUAL ACCOMPLISHMENTS

Table 1. Phase I Milestone Summary

MS#	Milestone Description	Milestone Type	Ant. Qtr.	Status
M1.1	SSE stable in dry room for 30 minutes	Technical	Q2	100% completion
M1.2	SSE ionic conductivity ≥10^{-4} S/cm	Technical	Q3	100%
M2.1	Film area ≥10 cm^2; SSE layer ≤ 100µm	Technical	Q4	100%
M3.1	Initial anode protection	Technical	Q3	100%
M4.1	Initial solid state cell assembled	Technical	Q4	100%
M5.1	Down select process parameters	Technical	Q5	100%
M5.2	Cathode loading ≥ 3.0 mAh/cm^2	Technical	Q6	100%
M6.1	SSE stable in dry room for 2 h	Technical	Q6	100%
M6.2	SSE stable 0 – 5 V	Technical	Q6	70%
M7.1	Film area ≥30 cm^2; SSE layer thickness ≤50 µm	Technical	Q6	60%
M8.1	Laminable protected Li anode	Technical	Q6	50%
M9.1	Solid state cell assembled (TRL 4)	Technical	Q6	20%
M9.2	Feasibility for a 400 Wh/kg cell	Go / No Go	Q6	100%
M9.3	Cycle life of ≥ 250	Go / No Go	Q6	40%

Table 2. Phase II/NCE Milestone Summary

Milestone	Status	Date
Task 1. SSE powder development		
SSE powder 4h air stability and 0.5 mS/cm	Completed	Q3, FY2019
SSE powder 8h air stability and 1 mS/cm	Completed	Q3, FY2020
Task 2. Cathode development		
Process down selection	Completed 90%	Q1 FY2022
Demonstrate 500 g cathode powder production	Completed	Q4, FY 2020
SSE $\geq$ 50 cm^2	Completed	Q3, FY2020
Task 3. Li anode development		
Li anode protection thickness $\leq$50 µm	Completed	Q4, FY2020
Li anode protection method verification		Q4, FY2020
Task 4. Cell stack development		
Cathode loading $\geq$ 3 mAh/cm^2	Completed in disk-type cell	Q1 FY 2020
SSE Film thickness $\leq$ 25 µm	In progress	Q1 FY 2022
SLP-DLP with free-standing cathode film	Completed	Q1 FY 2022
Task 5. Cell Assembly		
12 preliminary cell delivery	Complete. Disk-cell in pouch	Q3, FY2020
2.5 Ah pouch cell assembly	Challenging due to scale-up	Q1 FY 2022
12 final test cell delivery	Challenging due to scale-up	Q1 FY 2022
Task 6. Cell Test		
Cell specific energy of 500 Wh/kg	in progress	Q1 FY 2022
Cell cycle life of 1000	in progress	Q1 FY2022

Project Goal

Air-stable electrolytes will be synthesized and characterized, SSE powder with 4h air stability and 1 mS/cm will be down selected. Different active materials in cathode will be evaluated. Processes will be developed for initial cathode/SSE bilayer fabrication. Protected lithium metal anode development will be initiated and performed in parallel effort. Initial solid cells will be assembled and tested.

The SSE material will be optimized. Active materials in cathode will be down selected. Cathode fabrication process will be extended to all solid cathode/SSE/binder composite. Percentage of Active material/SSE/Binder in cathode will be finalized. Protected lithium anodes will be evaluated and laminated to the cathode/SSE composite. Interfacial impedance bottlenecks will be identified and resolved. All-solid-state cells will be assembled and tested to meet the target. Demonstrate that ASSB has a cell specific energy of 500 Wh/kg with a cycle life of 1000 cycles and assemble 2.5 Ah pouch cells.

Project Accomplishment

Phase I:

1. Key equipment and facility establishment

Both Navitas and partners have secured necessary equipment (facility) for solid state electrolyte synthesis, characterization, electrode and cell fabrication, and cell testing, including gloveboxes, ball mills, presses, XRD, Raman, SEM, cell assembly facility, and electrochemical test stations (Solartron and Maccor). Figure 1 shows some of the key capabilities deployed for solid electrolyte development.

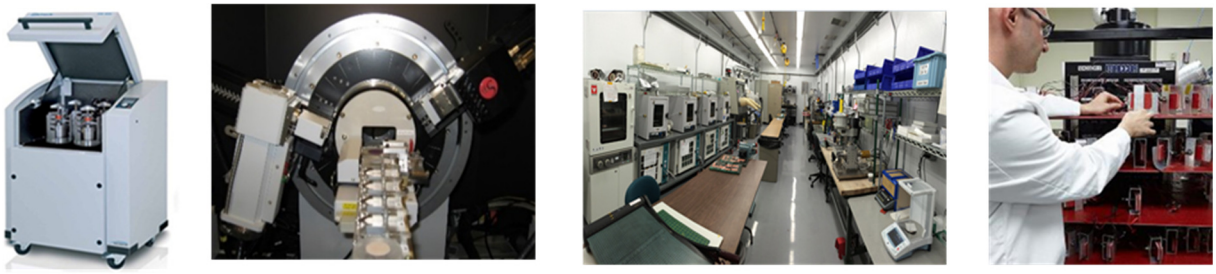

Figure 1: (from left to right) a ball mill for powder synthesis, a XRPD for powder structure analysis, a fully-equipped cell assembly facility, and a cell test station.

2. Solvent-free cathode fabrication

Navitas started with Li_2S powder as a LPS substitute to develop the SSB cathode fabrication process since (SSE) material is not available from UMD.

A lithium metal oxide powder (active material) was premixed with the sulfide. The ratio of active material to sulfide ranged from 9/1 to 7/3. The above composite cathode powder was further blended with carbon and dry polymer binder powder. The mixture was then calendered to form a cathode film. Figure 2 shows the solvent-free process for the composite cathode film fabrication.

At last, the stand-alone cathode film was laminated to Al foil to form cathode electrode through a calender machine (Figure 3).

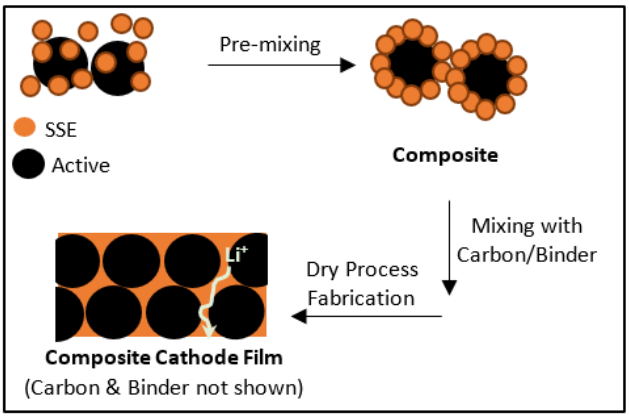

Figure 2. Schematic process to form a SSB composite cathode incorporated with SSE

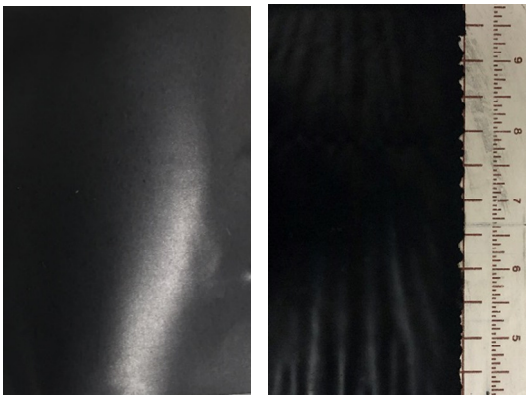

Figure 3. Pictures of a stand-alone cathode film (left) and a laminated cathode electrode (right)

3. The *Sulfide film fabrication*

solvent-free process was also developed to fabricate a Li_2S film (as the LPS substitute). The lithium sulfide powder was dry-blended with a polymer binder. The mixture was then calendered to form a film. Three samples have been tested in initial trials, with sulfide to polymer ratio of 90:10, 70:30, and 50:50, respectively. Stand-along films were fabricated successfully with thickness of 100 – 150 µm. The 90:10 film was brittle and the 50:50 film was very flexible. The 50:50 sulfide-polymer film is shown in Figure 4.

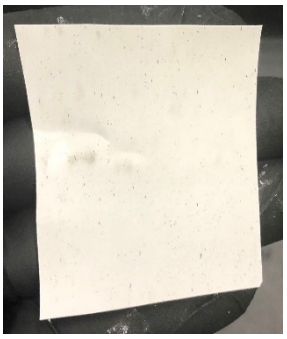

Figure 4. Picture of the 50:50 sulfide-polymer film

4. ***Air stable sulfide SSE development*****-----*$75Li_2S$-$25P_2S_5$ *(or* Li_3PS_4*, LPS)***

$75Li_2S$-$25P_2S_5$ (or Li_3PS_4, LPS) solid electrolyte has been developed with an ionic conductivity comparing to a liquid electrolyte. However, the LPS electrolyte reacts with water (moisture) in air. Doped LPS materials were developed at UMD, which showed stability of >30 minutes in the dry room (meeting Milestone 1.1).

The doped LPS materials were prepared by ball milling under argon for 2 hours. Two types of doping materials (A and B) were selected and the molar ratio of LPS to the dopant was set to 9:1.

The two doped LPS and the baseline LPS glass materials were characterized by XRD. The two doped materials showed the same amorphous patterns as the baseline LPS (Figure 5), confirming a homogeneous doping process.

The electrolyte powders were pressed into pellets and tested for ionic conductivity after exposed to the dry room air for 0, 30 and 90 minutes, respectively.

Before the exposure, both the doped electrolytes (with dopants A and B) showed ionic conductivity of > 0.25 mS/cm at room temperature. The electrolyte with "Dopant A" showed 9% conductivity reduction after 30 minutes exposure and 22% reduction after 90 minutes exposure. Meanwhile the electrolyte with "Dopant B" showed no conductivity change over the same exposure periods, indicating its structure stability in the dry room environment (Figure 6).

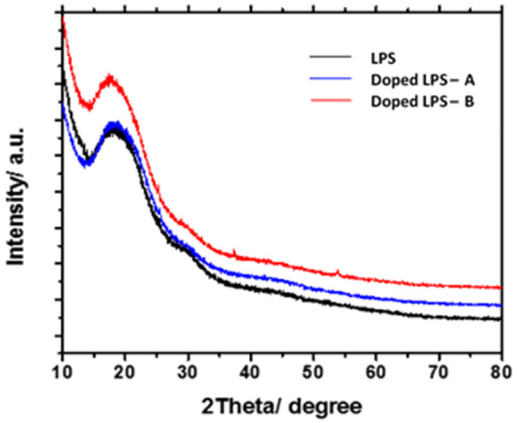

Figure 5. XRD patterns of LPS electrolytes before and after doping. The broad peaks between 10° to 40° are from the polymeric sample holder (background)

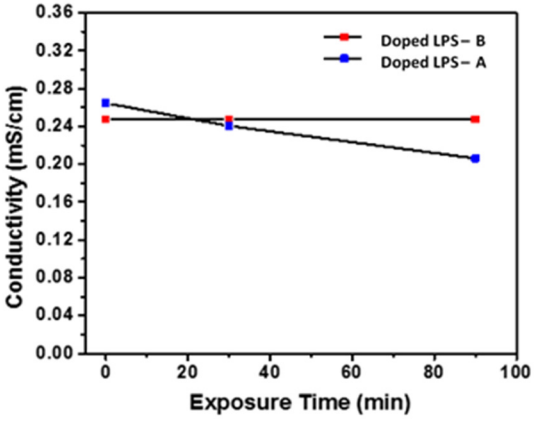

Figure 6. Ionic conductivity of two doped LPS materials after exposed to the dry room for 0, 30, and 90 minutes, respectively. Doped LPS-B met the stability milestone 1.1.

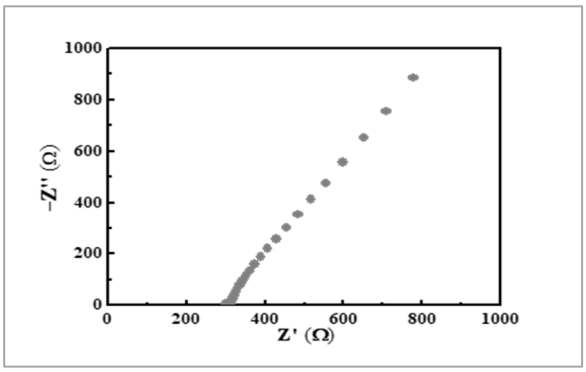

Figure 7. Impedance of LPS-B electrolyte. Its Li ion conductivity is calculated to be 0.3 – 0.4 mS/cm. It met the conductivity milestone 1.2 (> 0.1 mS/cm).

The ionic conductivity of LPS-B was measured to be 0.3 – 0.4 mS/cm. It met both air stability target (>30 minutes) and conductivity target (>0.1 mS/cm). The results are shown in Figures 7.

5. ***Li metal protection*** *-----LiPON coating by ORNL*

ORNL prepared and evaluated lithium coatings and solid electrolyte deposition on the lithium metal. **Figure 8** shows images of the deposited films. The left image is a picture of the as deposited lithium metal. The middle image is the lithium film with a thin coating of the solid electrolyte LIPON. The process was scaled-up to deposit the Li film from 2 cm × 2 cm to 6 cm × 8 cm in size (Fig. 8, right).

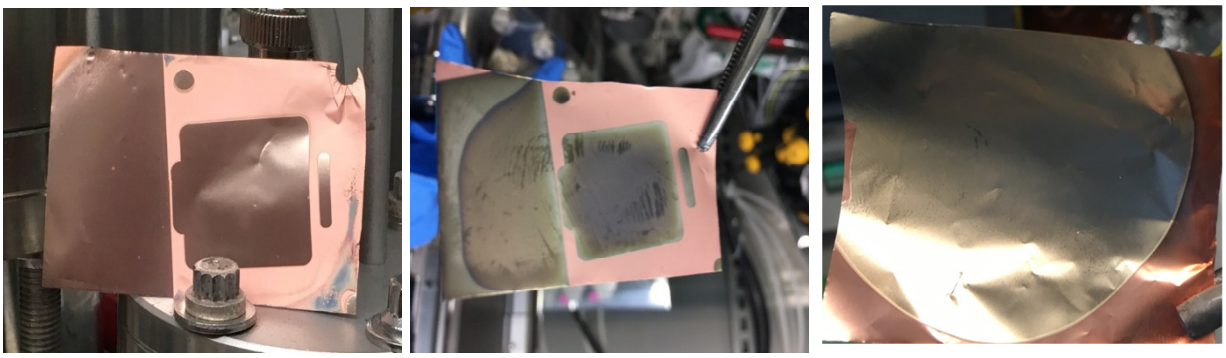

Figure 8. Images of deposited films: lithium metal deposition on Cu foil (left), LIPON deposition on Li film (middle, 2 cm x 2 cm), been scaled-up to 6 cm x 8 cm (right),

6. *Cathode / SSE bi-layer film fabrication*

A solvent-free process was developed to fabricate a cathode/SSE bilayer film by laminating the two stand-alone films with a calender machine. As shown in **Figure 9**, a bi-layer film with a 3 cm × 4 cm size has been laminated.

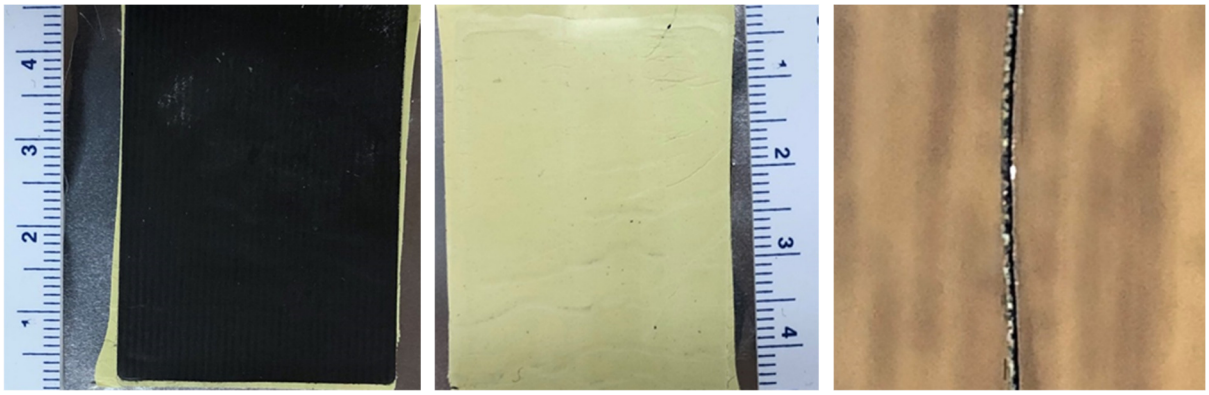

Figure 9. Images of the cathode / SSE bilayer film: view from cathode side, view from SSE side, and cross-section view (left to right)

7. ***Solid state cell fabrication and test***------*Swagelok cell and Single-Layer Pouch Cell.*

Lab scale Swagelok (Figure 10C) and Single-layer-pouch cells (Figure 10D) were assembled for a full cell demonstration.

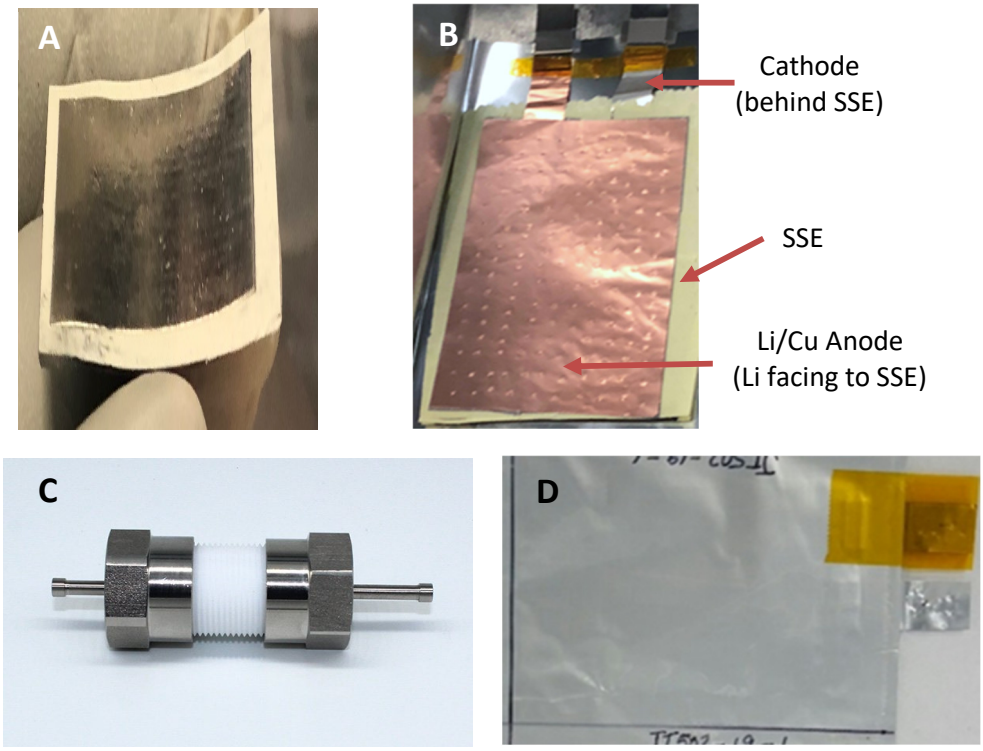

Figure 10. Figure 10. (A) Laminated cathode / SSE bilayer film and (B) dry stack of "Cu-Li / SSE / Cathode" to build pouch cells. Two types of cells were used to qualify the Li-SSE-cathode stack: (C) lab scale Swagelok cell; and (D) solid state pouch cell.

8. ***Solid state cell fabrication and test***------*Swagelok* ***LCO/LPS/Li*** *Cell*

Rate capability of the lab-scale Swagelok cell was conducted by charging it to 4.2V at 0.1C and discharging it to 2.5V at various rates up to 1C. It shows 83% capacity retention at 0.2C, 65% at 0.5C, 50% at 1C, respectively (**Figure 11**, right).

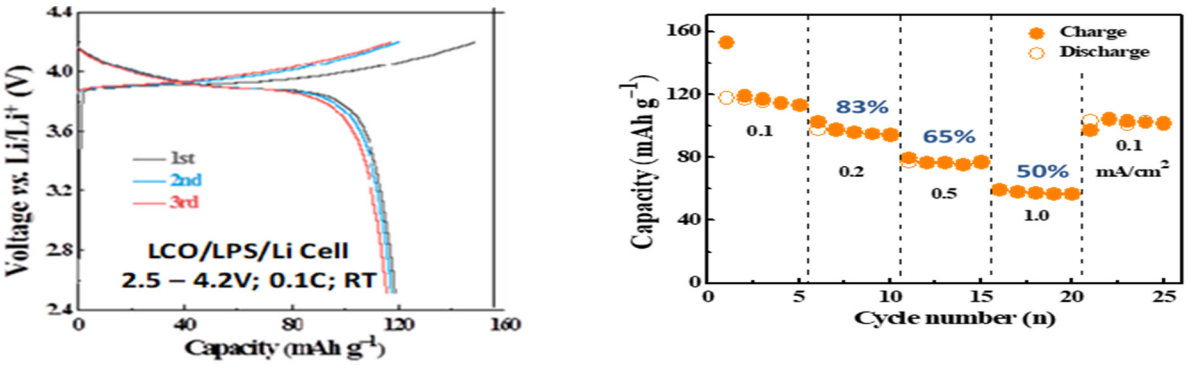

Figure 11. Charge-discharge profile of the Swagelok LCO/LPS/Li cell for the first 3 cycles (left). Rate capability of the Swagelok LCO/LPS/Li cell at room temperature (right). The cell was charged at 0.1C to 4.2V and discharged to 2.5V

The cell also shows very promising cycle life. It retained 83% of the initial capacity after 100 cycles so far (**Figure 12**; cycled at 2.5 – 4.2V, and room temperature)

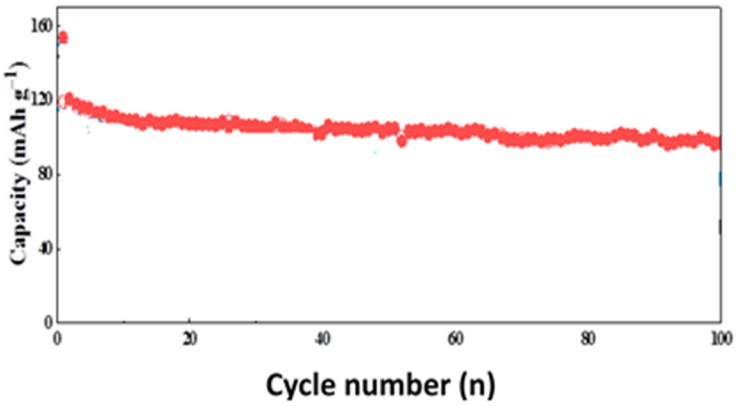

Figure 12. Cycle life of the LCO/LPS/Li cell at room temperature 2.5 – 4.2V). The cell retains 83% of initial capacity after 100 cycles.

*9. **Characterization and optimization of the interphase of SSE and Li**------LiF-rich SEI layer*

By introducing a LiF-rich SEI layer between the LPS SSE and the Li metal anode through coating/infiltrating LiFSI-DME into LPS, we significantly increased the critical current density of the LPS from 0.7 mA/cm^2 to a record-high value of > 2 mA/cm^2 at room temperature and dramatically enhanced the Li plating/stripping Coulombic efficiency from 88% to 98%.

The interphase morphology and composition Li metal and the SSEs were analyzed using SEM, Time-of-flight secondary ion mass spectrometry (ToF-SIMS) and X-ray photoelectron spectroscopy (XPS).

10. SEM Analysis of the interphase layers between the Li metal and LPS SSE

Figure 13a and 13b show the surface morphology of the cycled LPS recovered from Li|LPS|SS and Li|LiFSI@LPS|SS. The untreated Li_3PS_4 shows substantial cracking after prolonged cycling due to the side reactions ($Li_3PS_4 + 8Li \rightarrow Li_3P + 4Li_2S$) between Li metal and the solid-state LPS electrolyte, as evidenced by the low CE and poor cycling stability, which has been shown in the last report.

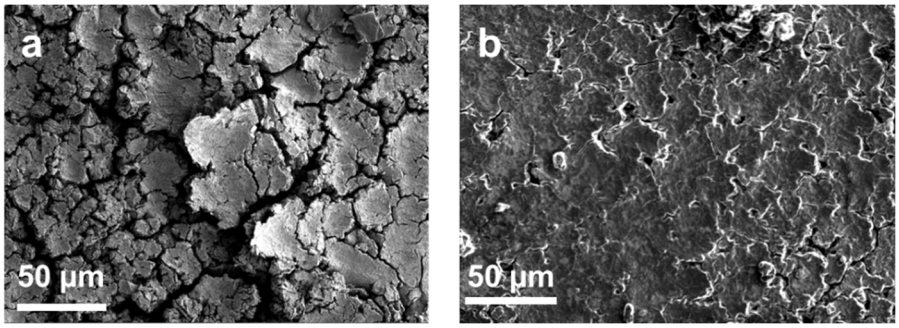

Figure 13. (a) SEM image of the cycled LPS recovered from untreated cell. (b) SEM image of cycled LPS recovered from pre-treated cell.

11. Phase diagram and calculations for the reactions between the Li metal and LPS SSE

Figure 14a shows the ternary phase diagram of the Li-P-S obtained from Materials Project (MP). The reaction between the Li_3PS_4 and Li metal will ultimately form the fully lithiated species of Li_2S and Li_3P, with LiP_7, Li_3P_7, LiP forming as possible intermediates. However, these reduction products cannot act as the effective SEI layers due to the high electronic conductivity of Li_xP (**Figure 14b**). The formation of lithiated layer will increase the Li content on the LPS surface.

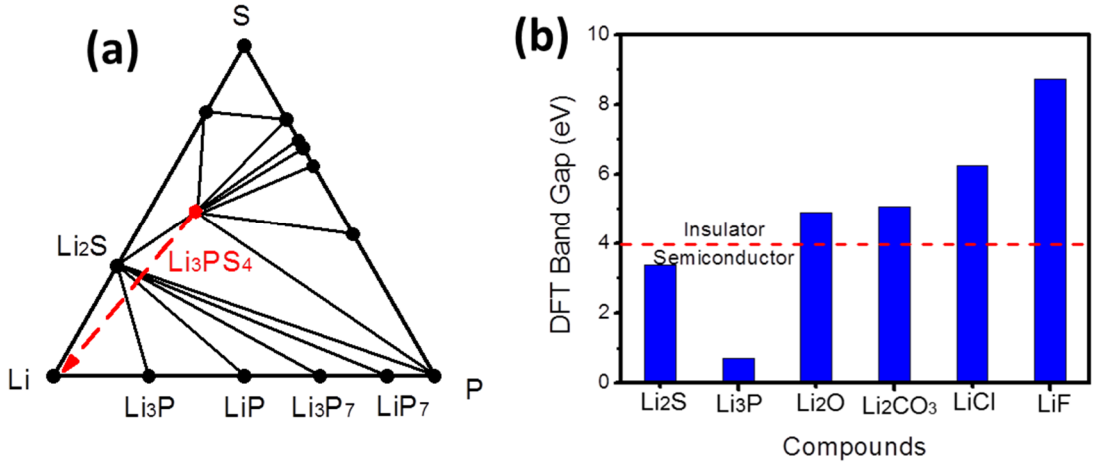

Figure 14. (a) Ternary phase diagram and (b) comparison of the Band gaps for different materials. Generally, 4.0 eV is regarded as the dividing line between the semi-conductors and the insulators. Obviously, the *in situ* formed Li_3P during Li plating/stripping is too conductive to block the electron transport in the as-formed passivation layers between the solid-state electrolyte and the Li metal because of the low band gap of 0.7 eV. The values are obtained from Materials Projects.

12. ToF-SIMS Analysis of the interphase layers between the Li metal and LPS SSE

ToF-SIMS analysis was used to map the Li content in the cross-section. As shown in **Figure 15**, the Li content in the cracked layer of the cycled LPS SSE was higher than that in the bulk LPS SSE, confirming the side reactions of LPS with Li.

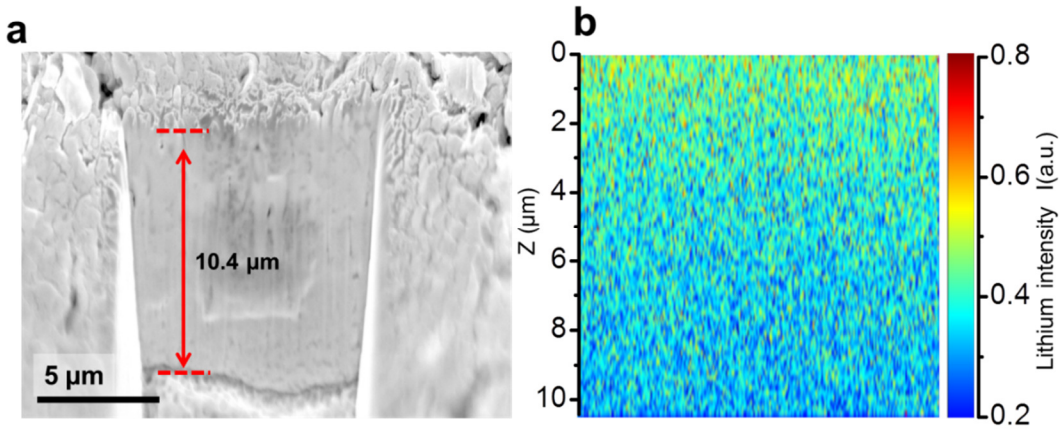

Figure 15. ToF-SIMS analysis of the positive ions for the interface of the Li_3PS_4. (a) SEM image of the cycled Li_3PS_4 SSE after Ga^+ beam sputtering; (b) the Li element distribution with depth.

Phase II:

13. ***Air stable sulfide SSE development*****------** *CaO doped LPS-P_2O_5 with improved air stability and conductivity*

Doping with oxides is one of the most effective strategies to improve the chemical stability of SSE. LPS-P_2O_5 glass-ceramic electrolyte, and CaO doped LPS-P_2O_5 electrolyte were prepared by ball milling at 230 rpm under Ar for 2 h. The molar ratio of LPS-P_2O_5 and CaO is set to be 95: 5.

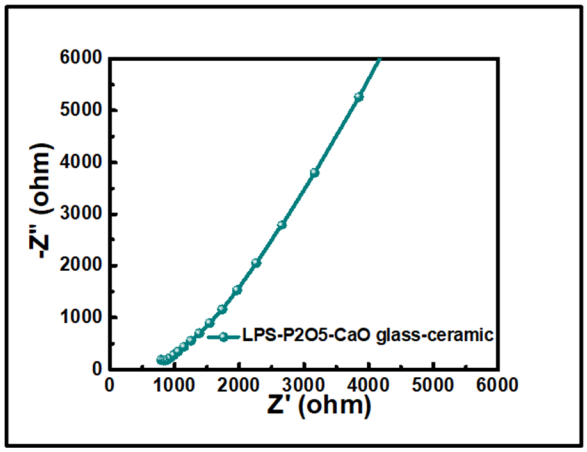

Figure 16. Impedance of LPS-P_2O_5-CaO electrolyte. Its Li ion conductivity is calculated to be 0.475 mS/cm. It almost meets the conductivity milestone 1.1 (> 0.5 mS/cm).

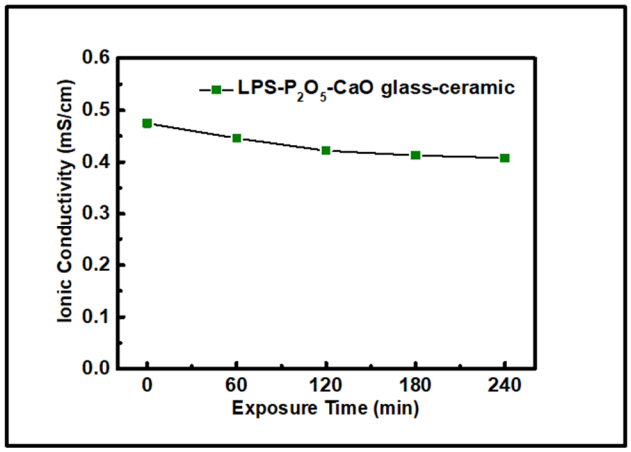

Figure 17. Ionic conductivity changes of the co-doped LPS materials after exposure to the dry room air up to 240 min.

The ionic conductivity of the co-doped electrolyte was measured to be 0.475 mS/cm (Figure 16). Besides, as shown in Figure 17, the selected co-doped LPS-P_2O_5-CaO electrolyte retains 86% of its initial conductivity after exposure of 4 hours in the dry room, indicating the significant improvement in air stability and conductivity.

*14. **Solid state cell fabrication and cycling performance**------Swagelok cell Li// LPS-P_2O_5-CaO//$LiCoO_2$*

In **Figure 18**, the disk-type Li-$LiCoO_2$ ASSB with LPS-P_2O_5-CaO glass-ceramic electrolyte shows an initial discharge capacity of 127.5 mAh g^{-1}. After the first two cycles, the Coulombic efficiency can reach a high value of 98.54% at the third cycle. The new designed LPS-P_2O_5-CaO solid electrolyte also shows very promising cycling life in full cell. It can retain a high capacity retention of 80.8% after 40 cycles.

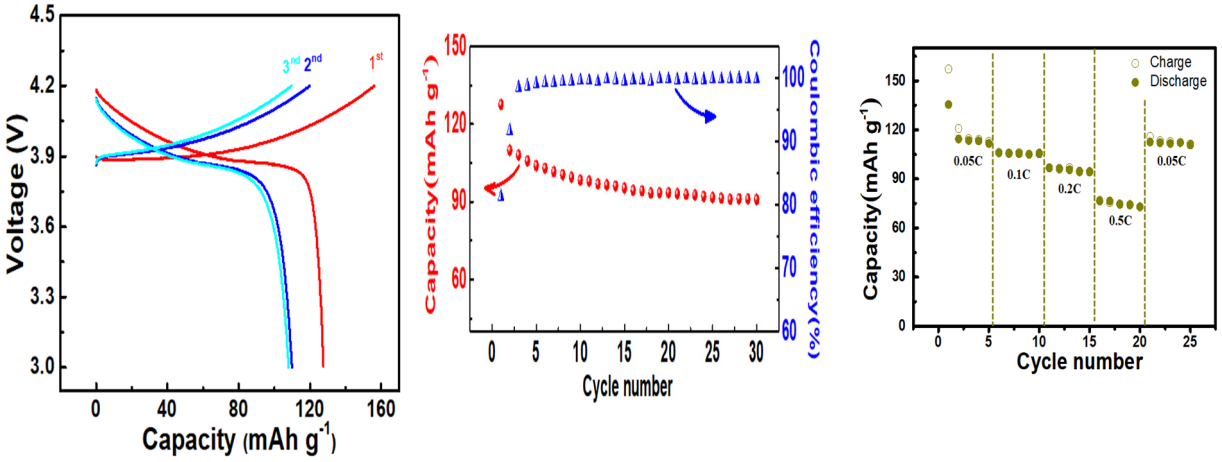

Figure 18. the Swagelok-type **LCO/LPS-P_2O_5-CaO /Li cell: Charge-discharge profile at 0.1 C of for the first 3 cycles (left); Cycle life at 0.1 C (middle); Rate capability (right). Tested between 3.0 – 4.2 V (1C = 120 mAh/g), at 60 °C.**

Rate capability test showed a high capacity retention of 105.5 mAh g^{-1} at 0.1C, 95.8 mAh g^{-1} at 0.2C, 75.2 mAh g^{-1} at 0.5C, respectively (**Figure 18**, right).

*15. **Characterization of CaO-doped LPS-P_2S_5**------- LPS-P_2O_5-CaO*

The SEM image (**Figure 19**) shows the pristine LPS-P_2O_5-CaO solid-state electrolyte particles have an average size ranging in 5-15 μm with irregular sharps.

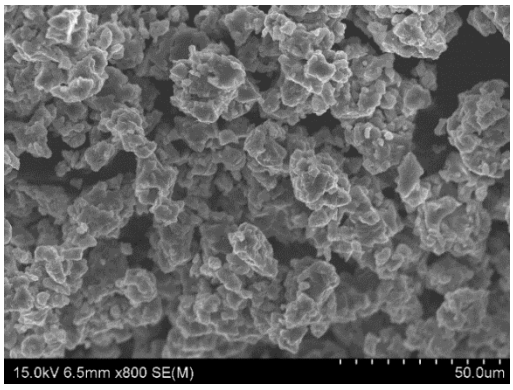

Figure 19. SEM image of LPS-P_2O_5-CaO solid-state electrolyte powder.

Figure 20 shows the Raman spectrum of the LPS-P_2O_5-CaO glass-ceramic powder. Only one characteristic peak of PS_4^{3-} ion at around 418 cm^{-1} is observed in the LPS-P_2O_5-CaO glass-ceramic, suggesting that a small amount of P_2O_5 and CaO added to the $75Li_2S{\cdot}25P_2S_5$ sulfide systems does not change the existence of PS_4^{3-} ion. Compared with other P-S groups (such as $P_2S_7^{3-}$, PS_3^{-}), PS_4^{3-} ion group exhibits the best chemical stability in air among the Li_2S-P_2S_5 binary systems, which also helps to make the fabricated LPS-P_2O_5-CaO glass-ceramic difficult to be hydrolyzed by H_2O molecules in the atmosphere.

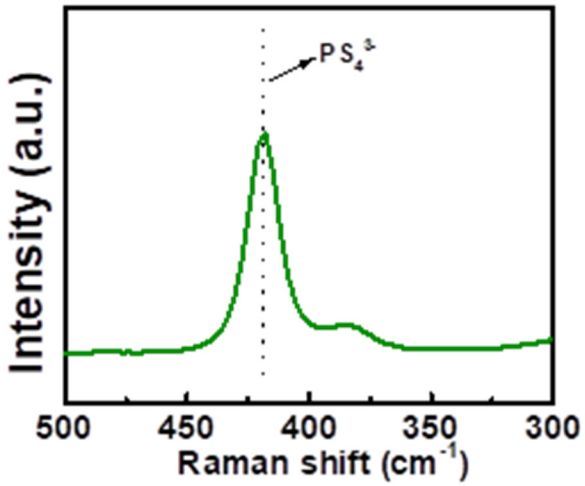

Figure 20. Raman spectrum of LPS-P_2O_5-CaO solid-state electrolyte powder.

The conductivities were further measured every 25 °C from 25 °C to 100 °C, and the results are shown in **Figure 21**. The conductivities of LPS-P_2O_5-CaO solid-state electrolyte increases gradually as the temperature increases. The ionic conductivity is 0.48 x 10^{-3} S cm^{-1} at room temperature. When the temperature is increased to higher than 50 °C, the conductivity can reach a high value above 1.0 x 10^{-3} S cm^{-1}. Furthermore, the activation energies (E_a) could be calculated according to the equation as follows,

$$\sigma = Aexp(-\frac{Ea}{RT})$$

Where, σ = ionic conductivity; A = pre-exponential factor; Ea =activation energy; R = gas constant (8.314 J·K mol^{-1}); T = absolute temperature (K). The obtained Arrhenius plot shows the activation energies (E_a) of LPS-P_2O_5-CaO solid-state electrolyte is around 29.50 KJ mol^{-1}.

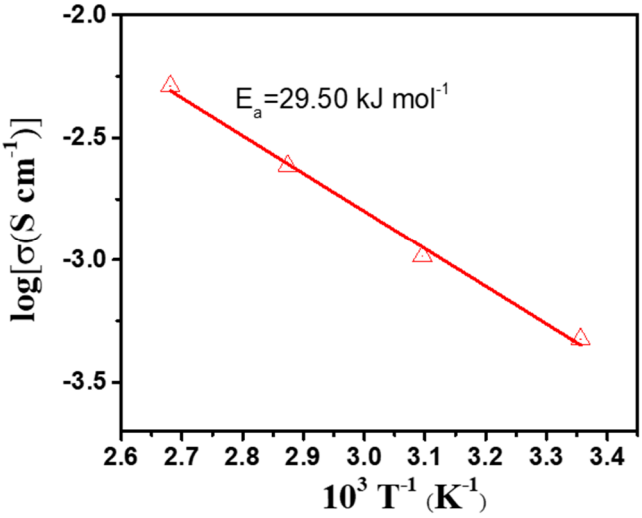

Figure 21. Arrhenius plots of LPS-P_2O_5-CaO solid electrolyte

Interface stability of Li metal and solid-state electrolyte------Critical Current Density Test

To initially evaluate the dendrite suppression capability of the LPS glass-ceramic electrolytes, Li/electrolyte/Li cells are assembled and tested by galvanostatic cycling at step-increased current densities. In a typical procedure of the Li/electrolyte/Li cell assembly, 120 mg solid electrolyte powder was pressed into a pellet under 360 MPa in a polytetrafluoroethylene (PTFE) tank with an inner diameter of 10 mm. After that, two 45 μm thick Li discs with a diameter of 10 mm were attached on both sides of the solid electrolyte film. The formed Li/electrolyte/Li cell was then sandwiched between two stainless steel rods which functioned as current collectors.

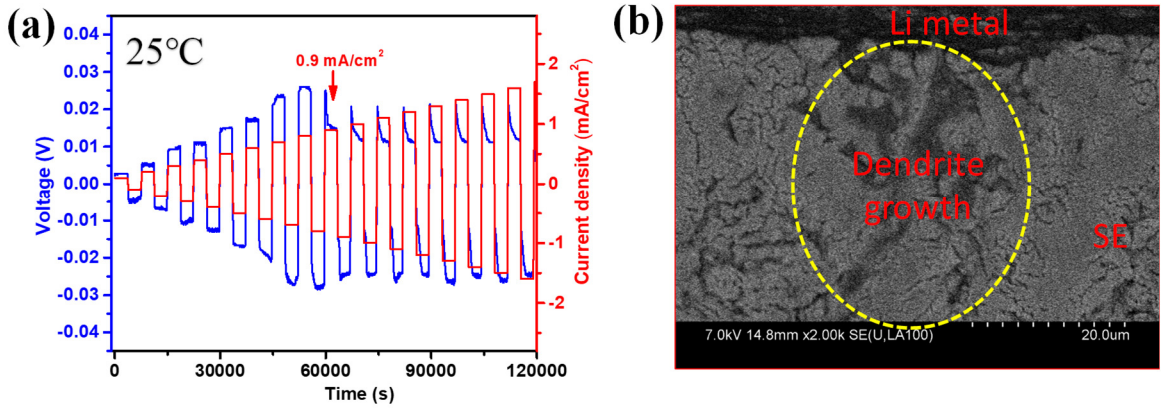

Figure 22. (a) Galvanostatic cycling of the Li-Li cells at step-increased current densities at 25 °C with LPS glass-ceramic solid electrolyte; (b) The backscattering electron images of the interface between Li metal and SE after Galvanostatic cycling.

The assembled cells were subjected to a galvanostatic cycling test at step-increased current densities both at 25 °C and 60 °C. **Figure 22a** shows the voltage-time profiles of LPS glass-ceramic at room temperature. Initially, the voltages increased with currents. After cycling for a certain amount of time, the Li-Li cells experienced a voltage drop at 0.9 mA cm^{-2}, which means the critical current density and capacity for the working solid electrolyte is 0.9 mA cm^{-2} of 0.9 mAh cm^{-2}. The voltage drop is considered

as a result of lithium dendrite formation in the solid electrolytes, as can be observed from the backscattering electron images. Since Li is a much lighter element, backscatter electrons of Li-dendrite area appear darker in the image (**Figure 22b**).

Since the high temperature operation is one important advantage for all-solid-state lithium batteries, the effects of temperature on the critical current densities of LPS glass-ceramic is also investigated. As shown in **Figure 23**, the critical current density and capacity for the LPS glass-ceramic solid electrolyte at 60 °C is around 1.5 mA cm^{-2}.

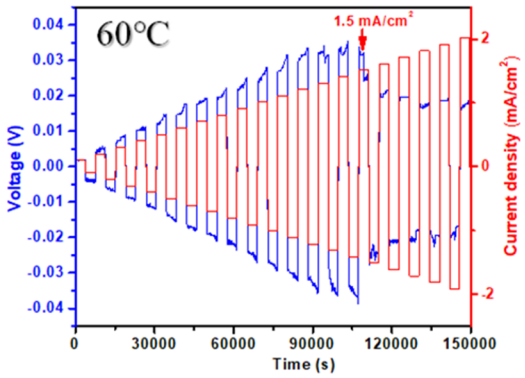

Figure 23. Galvanostatic cycling of the Li-Li cells at step-increased current densities at 60 °C with LPS glass-ceramic solid electrolyte.

16. Solid-state Li-S cell assembly

During this period, a solid-state battery with Li_2S composite/LPS/Li structure was fabricated and tested, in which a Li_2S composite cathode was used due to its high capacity and stability on the interface with LPS electrolyte. The solid-state Li-S batteries have several advantages comparing to the regular Li-S batteries using liquid electrolyte. As we all know, though Li-S battery is very attractive due to its superior energy density, the polysulfide shuttle effect significantly lowers its performance. Compared with Li-S batteries using ether-based liquid electrolytes, the shuttle effect in solid-state Li-S batteries can be radically avoided via eliminating polysulfide intermediates through solid-phase Li-S redox reaction of solid electrolyte.

For preparing the Li_2S cathode composite, a powder mixture consisted of Li_2S active materials, vapor grown carbon fiber (VGCF) and LPS solid electrolyte in a weight ratio of 55: 15: 30 was mechanically milled at 300 rpm for 10 h. To assemble the cell, Li_2S composite powder was put on one side of the LPS glass-ceramic solid electrolyte (~120 mg) membrane in a PTFE tank with a diameter of 10 mm, then cold-pressed together under 360 MPa pressure between two stainless steel rods, which act as the current collectors. Afterwards, a Li foil with diameter of 8 mm were placed on the other side of the solid electrolyte membrane and the cathode/LPS/Li film was pressed between two stainless steel rods by hand.

Galvanostatic charge-discharge cycles were conducted at 0.05C in a voltage range of 1.2-3 V at room temperature. The current density and specific capacity in this report were calculated based on the weight of Li_2S (1C=1160 mAh g^{-1}). As shown in **Figure 24**, the Li-Li_2S ASSB with LPS glass-ceramic electrolyte

showed an initial discharge capacity of 671.6 mAh g^{-1}. After the first cycle, the Coulombic efficiency reached a high value of 96% at the second cycle.

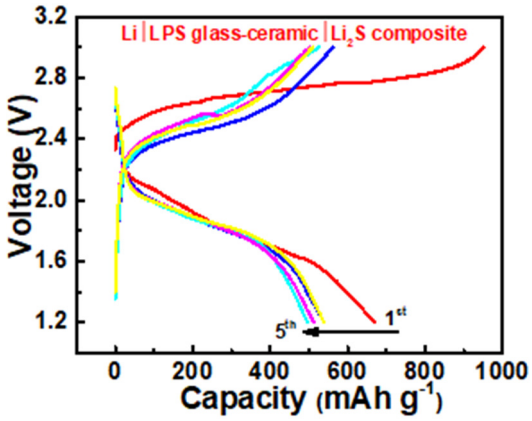

Figure 24. Charge-discharge profile of the Li_2S/LPS glass-ceramic /Li cell for the first 5 cycles. It was measured at 0.05 C, 1.2-3 V and room temperature.

Li_2S composite cathode with up to 3.13 mAh cm^{-2} loading has been tested in full solid-state cell with LPS glass-ceramic electrolyte to meet milestone 4.1 of >3 mAh cm^{-2} cathode. For preparing the Li_2S composite cathode, a mixer containing Li_2S active materials, vapor grown carbon fiber (VGCF) and LPS solid electrolyte in a weight ratio of 55: 15: 30 was firstly mechanically milled at 300 rpm for 10 h. To assemble the Li@20μL 6FD /LPS glass-ceramic /Li_2S cell, Li_2S composite powder was put on one side of the LPS glass-ceramic solid electrolyte (~120 mg) membrane in a PTFE tank with 10 mm diameter in a Swagelok cell, then cold-pressed together under 360 MPa between two stainless steel rods, which would act as the current collectors. Afterwards, 20μL of 6M LiFSI DME (6FD) were added on the other side of the solid electrolyte membrane, and a Li foil with diameter 8 mm were attached and dried at 120°C under vacuum overnight.

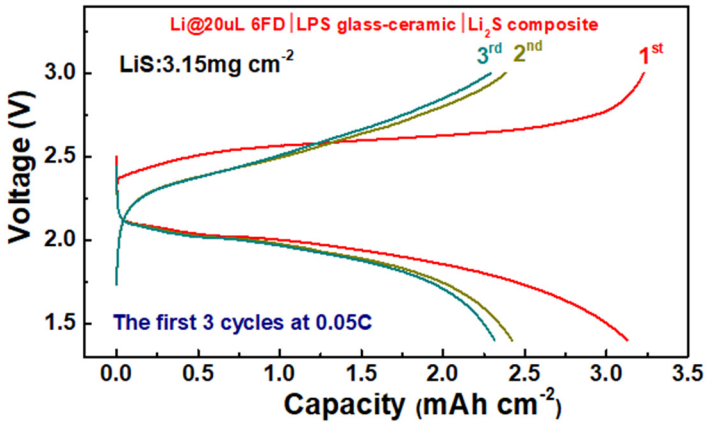

Figure 25. Charge-discharge profile of the Li@20μL 6FD /LPS glass-ceramic / Li_2S cell for the first 3 cycles. It was measured at 1.4-3 V and at 0.05 C at room temperature.

The first three cycling performance with Li_2S loading of 3.15mg cm^{-2} can be found in Figure 1. As shown in the figure, the Li-Li_2S all solid-state battery (ASSB) with LPS glass-ceramic electrolyte exhibited a high initial discharging capacity of 3.13 mAh cm^{-2} with a Coulombic efficiency around 89.6%. The 20µL 6M LiFSI DME electrolyte that was added between Li metal anode and LPS electrolyte, can form a LiF-rich SEI to suppresses lithium dendrite into the solid electrolytes. After the first cycle, the discharge capacity can also maintain a high value of 2.42 and 2.31 mAh cm^{-2} at the second and third cycle, respectively.

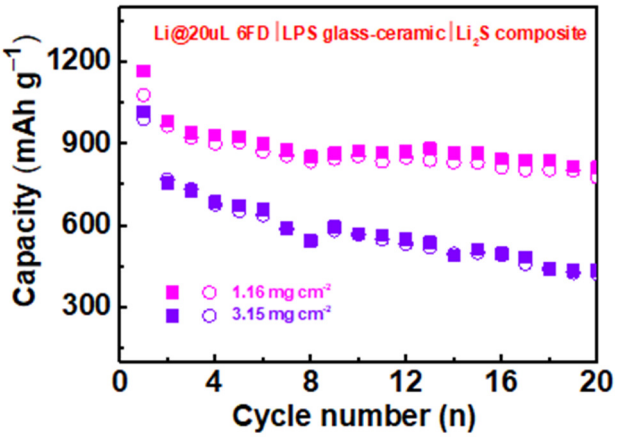

Figure 26. The cycling performance of the Li@20µL 6FD /LPS glass-ceramic / Li2S cell with different Li2S loading . It was measured at 1.4-3 V and at 0.05 C at room temperature.

The cycling performance of different Li_2S loading was also tested and compared under room temperature. As shown in Figure 26, at a low loading of 1.16 mg cm^{-2} Li_2S, the Li-Li_2S ASSB with LPS electrolyte showed an initial discharging capacity of 1077.5 mAh g^{-1} (areal capacity was 1.25 mAh cm^{-2}). After 20 cycles, the capacity maintained around 776.3 mAh g^{-1}. For the cell with a high loading of 3.15 mg cm^{-2} Li_2S, it could also deliver a high capacity of 990.4 mAh g^{-1} in the first cycle. But during the following cycles, the areal capacity gradually faded to nearly 42.5% after 20 cycles. Hence, more research in high-energy-density ASSBs with long-term cycling and stable capacity retention are needed.

17. Thin Li metal anode Qualification------50 µm thick double-side lithium foil on Cu substrate

To reach the 500 Wh/kg cell specific energy, 50 µm lithium foil would be used in the pouch cell. We have tested a 50 µm thick double side lithium foil supported by Cu foil (Figure 27) in regular cells using liquid electrolyte, The results approved that the thin lithium has a good quality.

Figure 27. Photo of a roll of the 50 µm thick double-side lithium foil on Cu substrate for large format solid-state batteries.

18. Cathode film and stack------Li//LPS//LCO

Previously we have successfully developed a free-standing cathode film (LCO as an example and the process can be extended to other active materials) and LPS solid-state electrolyte (SSE) films, but in which the PTFE binder content normally was high (up to 30 wt%) to achieve a good mechanical strength and flexibility (**Figure 28 A-D**).

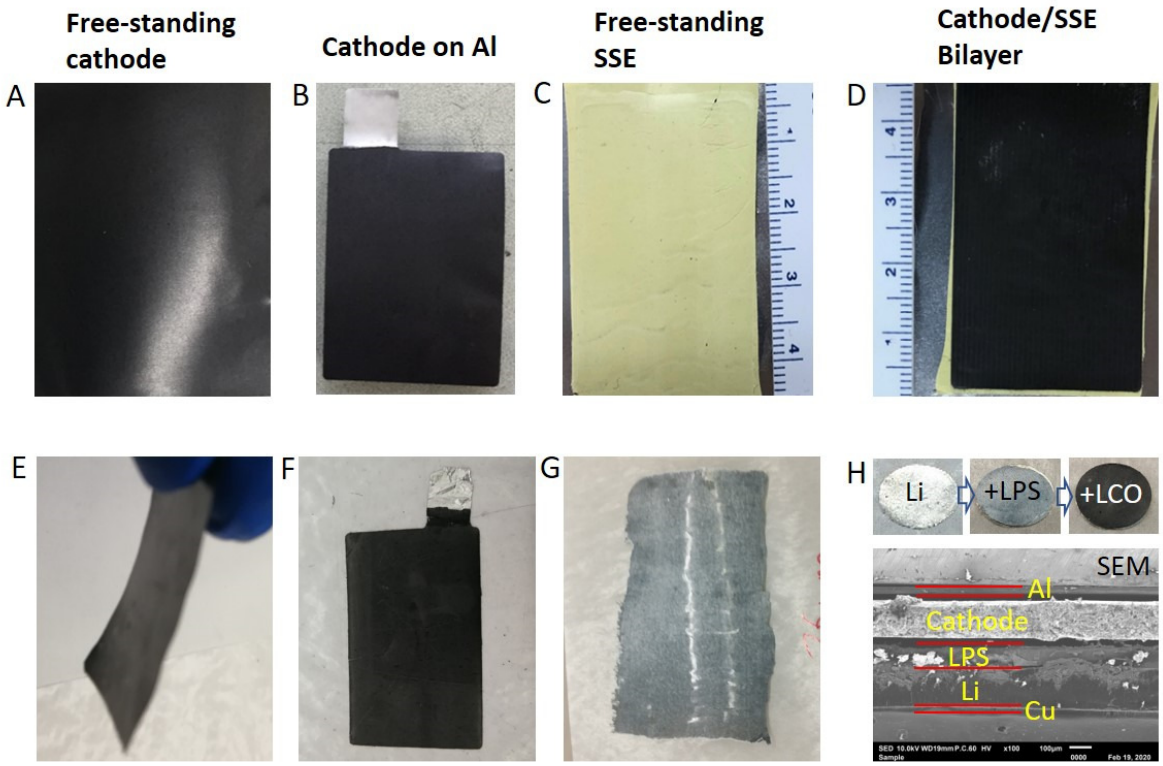

Figure 28. Images of free-standing LCO cathode composite film, cathode on Al foil, free-standing LPS composite solid-state electrolyte (SSE) film and cathode/SSE bilayer or cathode/SSE/Li stack. Top line images (A, B, C, D) contain 30 wt% PTFE, bottom line images (E, F, G, H) contain 10 wt% PTFE.

By adding 4 wt% of carbon promoter (which can replace a portion of carbon black that normally used in cathode formulation to make a total carbon content < 7 wt%) to an LCO cathode composite, a ~170 µm thick free-standing LCO cathode film (**Figure 28E**) prepared by knife blending following by roll-mill showed good mechanical strength and flexibility with only 5-10 wt% of PTFE binder (possible to lower to 2.5 wt%). It can be laminated to Al foil (**Figure 28F**) by roll-mill between room temperature and 120 ºC. The cathode film showed enough robustness to support the SSE film while we were preparing small cell stack sample. The loading of the LCO cathode was calculated to be ~4.5 mAh cm^{-2}, above the 3.0 mAh cm^{-2} target. This dry electrode process can be extended to high-loading NMC811 and Li_2S cathode.

The high content of polymer binder will lower the ionic conductivity of both SSE and cathode composites. The formulation and the process of SSE and cathode composite with a lower the binder content needs to be optimized while maintaining a relatively good mechanical strength and film.

*19. **Interface stability of Li metal and solid-state electrolyte**------Li//LPS//Li cell with **6 M LiFSI/DME***

120 mg solid electrolyte powder under 360 MPa in a polytetrafluoroethylene (PTFE) tank with a diameter of 10 mm, was sandwiched by two 45 µm thick Li discs and then two stainless steel rods to form *Li//LPS//Li symmetric cell*. When cycling the cell with a step-increased current density at room temperature, the Li-Li cells experienced a voltage drop at 0.9 mA cm^{-2} (**Figure 29a**), meaning the critical current density and capacity for the working solid electrolyte is 0.9 mA cm^{-2} of 0.9 mAh cm^{-2}. The voltage drop was considered as a result of lithium dendrite formation in the solid electrolytes, as can be observed from the backscattering electron images (**Figure 29b**).

To confirm that 6 M LiFSI/DME (6FD) electrolyte treatment on the interface of Li/LPS SSE can form a LiF-rich protection layer and improve the Li/LPS interphase stability, various amount of 6FD was used to treat the Li|LPS|Li solid-state cell and the same step-increased current density test was performed.

Figure 29c showed the voltage profiles of Li@**10µL** 6FD-LPS-Li@10µL 6FD cell at a fixed half cycle of 0.5 h but a step-increased current density. Initially, the cell showed a similar trend of increase in Li plating/stripping overpotentials with the increment of the current density. As the current density increased to 1.1 mA cm^{-2}, a sudden voltage drop was observed at the 29th cycle in the cell because of the dendrite penetration into the SSE.

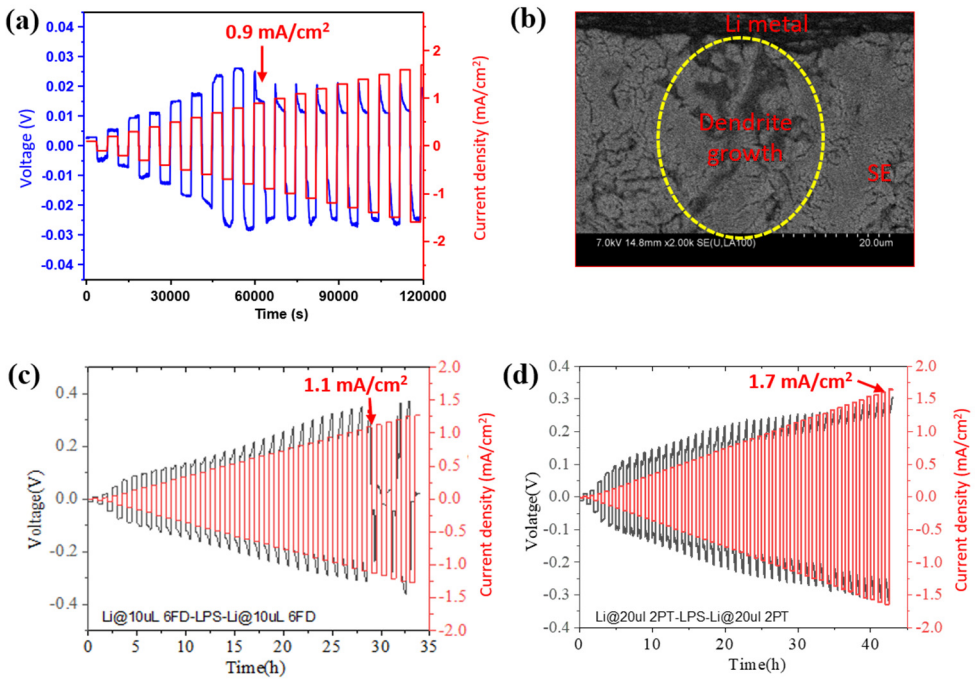

Figure 29. (a) Galvanostatic cycling of the Li-Li cells at step-increased current densities at 25 °C with LPS glass-ceramic solid electrolyte; (b) The backscattering electron images of the interface between Li metal and SE after Galvanostatic cycling. (c) Galvanostatic cycling of the Li@10µL 6FD-LPS-Li@10µL 6FD cells at step-increased current densities at 25 °C. (d) Galvanostatic cycling of the Li@20µL 6FD-LPS-Li@20µL 6FD cells at step-increased current densities at 25 °C.

Meanwhile, no voltage drop could be observed for the Li|LPS|Li cell with **20 µL** 6FD treatment, even when the current density was increased to 1.7 mA cm^{-2} (**Figure 29d**). This was because the in situ-formed thin LiF-rich SEI was tightly contacted with both Li and LPS and the high interfacial energy of LiF with

Li metal (73.28 meV/Å^2) promoted Li^+ migration along the LiF surface rather than the dendritic plating. These results clearly demonstrated that 6FD modification to in-situ form a LiF-rich SEI layer at the interface of LPS SSE and the Li metal can significantly increase the critical current density, lower the resistance and suppress the Li dendrites growth.

To prove the long-term cycling performance, Li/LPS solid electrolyte/Li cells with 20μL 6FD electrolyte treatment are assembled using Swagelok cells and tested by galvanostatic cycling at R.T..

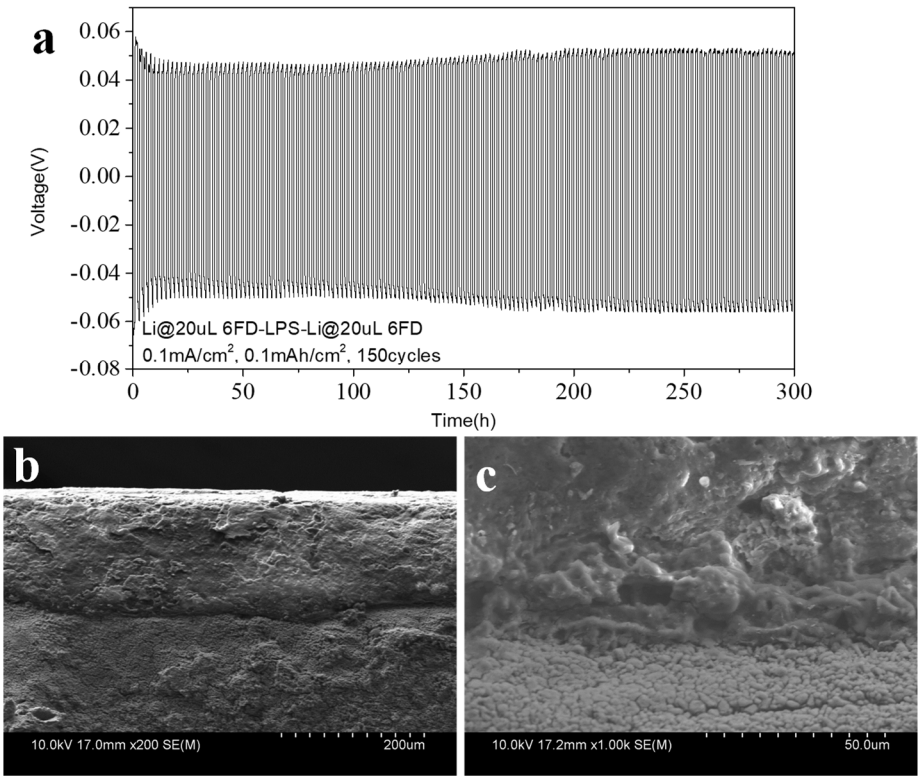

Figure 30. (a) Galvanostatic cycling of Li plating/stripping profiles in the Li@20μL 6FD-LPS-Li@20μL 6FD cells at a constant current density of 0.1 mA cm^{-2} at 25 °C; (b-c) The scanning electron microscopy (SEM) images of the interface between Li metal and SE after Galvanostatic cycling after 50 cycles at 0.1 mA cm^{-2}.

The cycling performances of the symmetric Li@20μL 6FD-LPS-Li@20μL 6FD cell was also tested at a current density of 0.1 mA cm^{-2} with a capacity of 0.1 mAh cm^{-2} at room temperature. As revealed in **Figure 30a**, the protected Li metal has run for more than 150 cycles with stable profiles. No clear voltage drop was observed, which meant LiF-rich SEI successfully suppressed lithium dendrite formation in the solid electrolytes. The scanning electron microscopy (SEM) images (**Figure 30b-c**) of Li/SSE interface were further characterized after 50 cycles at 0.1 mA cm^{-2}, which also showed a rather dense and smooth interphase without any cracking after prolonged cycling. Such a stable interphase of Li metal anode should help to improve cycling stability in full cells.

20. Solid-state Li metal cell assembly-------*novel disk-in-pouch tri-layer LCO/LPS/Li cell*

Due to the limited amount of LPS caused by ball mill repairing, we were using small amount of LPS for pouch cell size SSE film and cathode film development and optimization, but didn't use them for cell

performance test. Instead, we still use Swagelok cell (**Figure 31A**) as major cell type, but successfully extended to coin cell (**Figure 31B**) and a novel disk-in-pouch cell (**Figure 31C**) to simulate the pouch cell condition.

To simulate the pouch cell (**Figure 31D**) performance better using small amount of materials, we have tried to assemble the small tri-layer LCO/LPS/Li disk into a pouch cell. The tri-layer LCO/LPS/Li disk was the same with that in coin cell. In a typical process, the cathode/SSE bilayer film was prepared in a stainless-steel die with a chamber in 10 mm diameter under 360MPa following the similar procedure for solid-state coin cells. A Li metal disk was attached to the exposed SSE face and pressed to form a tri-layer stack. The stack was assembled into a pouch cell fixture for performance test (**Figure 31C**).

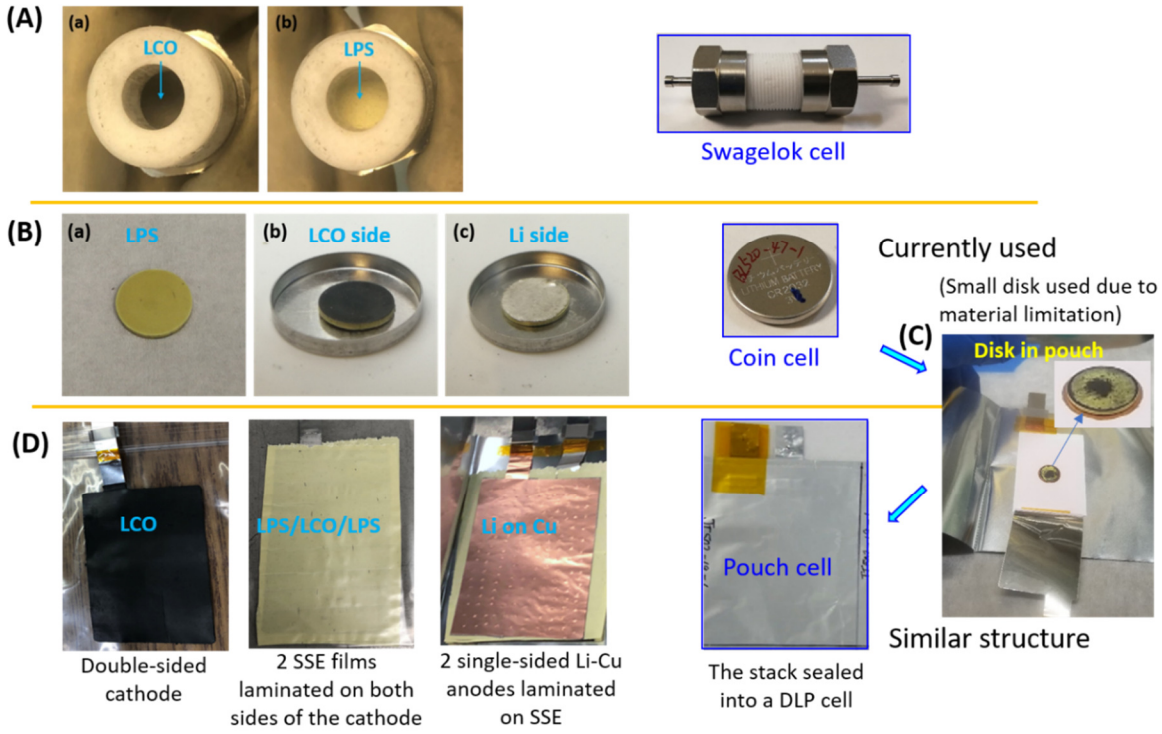

Figure 31. Solid-state cells in (A) Swagelok cell, (B) CR2032 coin cell, (C) disk-in-pouch cell, and (D) double-layer pouch cell format.

The pressure inside the disk-in-pouch cells seemed to have a big effect on the cell performance.

21. Ionic-conductivity stability of sulfide SSE in dry air------8-hour stability of LPS- P_2O_5-CaO

We further tested the 8-hour stability of LPS- P_2O_5-CaO electrolyte in dry air. The synthesis method: a mixture of 71 mol % of lithium sulfide (Li_2S), 25 mol% of phosphorus pentasulfide (P_2S_5) and 4 mol% Phosphorus pentoxide (P_2O_5) was milled in a 50 mL zirconia (ZrO_2) jar, at a fixed rotation speed of 500 rpm for 40 h. The obtained powder was then heated at 270 °C for 1 h in Ar for annealing to prepare the LPS-P_2O_5 glass-ceramic electrolyte. After that, CaO powder was mixed with LPS-P_2O_5 electrolyte by ball milling at 230 rpm under Ar for 2 h. The molar ratio of LPS-P_2O_5 and CaO was set to be 95: 5.

The ionic conductivity of electrolyte was measured by electrochemical impedance spectroscopy (EIS). Generally, 120 mg electrolyte powder was placed in the Swagelok cell and firstly pressed by applying pressure on the two steel ends by fingers, which was then pressed by the machine under the pressure around 360 MPa. The EIS frequency range was controlled between 10^7-1 Hz. As seen in **Figure 32A**, the

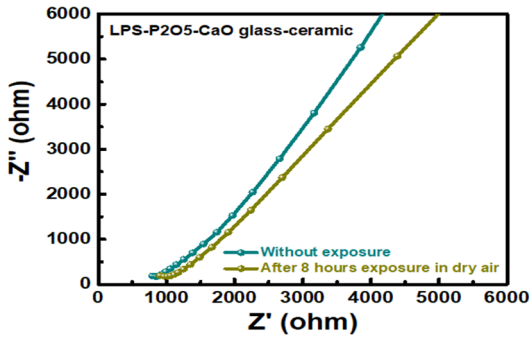

Figure 32A. Impedance of the original LPS-P_2O_5-CaO electrolyte and after exposure in dry air for 8 hours.

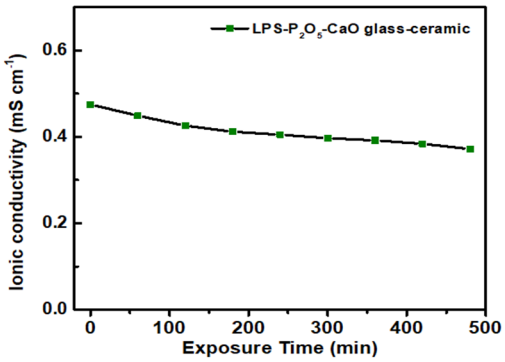

Figure 32B. Ionic conductivity change of the co-doped LPS-P_2O_5-CaO electrolyte after exposure to the dry air up to 480 minutes.

impedance of the bulk LPS-P_2O_5-CaO has been increased by 12% after 8 hours exposure in dry air. The specific trend of ionic conductivity was shown in Figure 32B. The initial ionic conductivity of the electrolyte was measured to be 0.48 mS/cm at beginning. The value was decreased to 0.41 (85%) and 0.37 mS/cm (77%) after 4 h and 8h exposure in dry air, respectively. The result confirmed the long-time air-stability of LPS-P_2O_5-CaO solid electrolyte, which still retained 77% of its initial ionic conductivity after exposure of 8 hours in the dry air.

22. ***Cell performance of sulfide electrolyte after air exposure*** *------ LCO/ LPS-P_2O_5-CaO/Li*

To further test the electrochemical performance of the solid electrolyte after air exposure, the Li-$LiCoO_2$ cells were tested with LPS-P_2O_5-CaO electrolyte that was exposed in dry air for 8 hours. Herein, surface-coated $LiCoO_2$ was used as cathode, and pure Li metal foil were used as the anode.

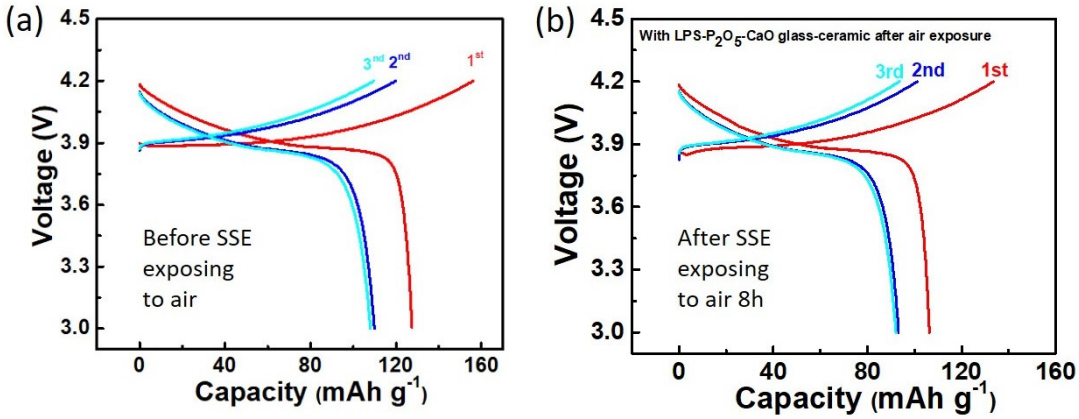

Figure 33. Charge-discharge profiles of the LCO/LPS-P_2O_5-CaO/Li cell for the first 3 cycles (a) before and (b) after LPS-P_2O_5-CaO was exposed in dry air for 8 hours. It was measured at 3.0 – 4.2 V and at 0.1 C, 60 °C.

As shown in the voltage profiles of LCO/ LPS-P_2O_5-CaO/Li cells using SSE before (**Figure 33a**) and after (**Figure 33b**) exposing to dry air for 8 hours, even after air-exposure up to 8 hours, LPS-P_2O_5-CaO glass-ceramic electrolyte still enables the Li-$LiCoO_2$ ASSB to display an initial discharge capacity of 106.3 mAh/g (83% of the initial discharge capacity for SSE before exposing to air in Figure 33a). After the first two cycles, the Coulombic efficiency reached to a high value of 98.4% at the third cycle (Coulombic efficiency was 98.5% before SSE exposed to air in Figure 33a). Therefore, the designed LPS-P_2O_5-CaO solid electrolyte showed excellent air stability and promising application in full cell.

28. Scaling up of LPS SSE synthesis

We have successfully scaled up the LPS SSE synthesis to 32g/jar and 128g/batch, eliminated the bottleneck of the large-scale preparation of SSE film and cathode composite.

29. Cathode materials investigation------surface-coated s-NCM622/LPS/Li cell

A higher specific capacity cathode material is desired for the 500 Wh/kg goal, high-Nickel NCM622 and NCM811 are still our cathode candidates. However, due to the stability issue, we were majorly working on LCO cathode and have never succeeded on a solid-state battery with NCM cathode. Though we have developed a >3 mAh/cm^2 Li_2S cathode during last report period, we were still working on the development of high capacity NCM cathodes. A big progress was made on solid-state batteries with a commercially available surface-coated NCM622 cathode.

The first cycle performance of SSB with 1.6 mAh/cm^2 surface-coated NCM622 (s-NCM622) composite cathode can be found in **Figure 34**. As shown in the figure, the first specific charge capacity was 185.1 mAh/g and first discharge capacity was about 126.5 mAh/g. The first Coulombic efficiency was about 68%. Considering the cell was not optimized with no stabilizer in SSE and the cathode composite containing polymer binder and carbon additives already (which decreases the ionic conductivity), the s-NCM622 seems a promising cathode candidate.

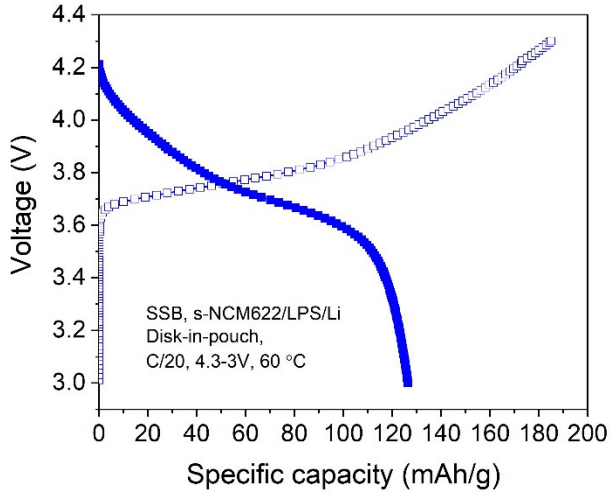

Figure 34. Charge-discharge profiles of the s-NCM622/LPS/Li disk-in-pouch cell for the first cycle. It was measured at 3.0 – 4.3 V and at 0.1 C, 60 °C.

*30. **Cathode composite film**------ s-NCM622-LPS-**PTFE**-Carbon 1-Carbon 2 = 70/24/**3**/1/2*

The formulation of s-NCM622 cathode composite powder was similar to previous LCO cathode composite but had some improvement. The active cathode content increased from 60% to 70% by weight, which could increase the capacity in cell level. The polymer binder was decreased from 10% to 3%, which could improve the ionic conductivity and increase the cell capacity, too. The final cathode formulation was "s-NCM622-LPS-**PTFE**-Carbon 1-Carbon 2 = 70/24/3/1/2, wt%".

We compared the two processing methods: (1) grinding in a mortar on the cathode/LPS for initial tests, (2) blending in a blender that we used for larger scale dry process cathode fabrication. In **Figure 35**, we showed the SEM images and EDAX mapping results of two films: SSE composite film prepared by grinding in a mortar with a pestle (**Figure 35a-d**) and cathode composite film prepared by blending in a blender (**Figure 35e-h**). Though the active materials were not exactly same (LPS only in SSE composite film and LPS/LCO mixture in cathode composite film), the other contents had the same weight ratio (3% PTFE, 3% total carbon additives), therefore the two films were fairly comparable.

Both methods seemed to disperse active materials well, indicated by the uniform distribution of LPS in S-mapping (**Figure 35d, 35h**). However, as you can see from **Figure 35b**, the carbon in the SSE film prepared by grinding was majorly aggregated on the surface, indicating the carbon was not dispersed well in the film by grinding method. The binder seemed aggregated into a large block in **Figure 35c**, indicating a poor dispersion and low film strength. In contract, the carbon dispersed all through from top to bottom in **Figure 35f** of the film prepared by blending method. There was no big block of PTFE binder indicated by F-mapping in **Figure 35g**.

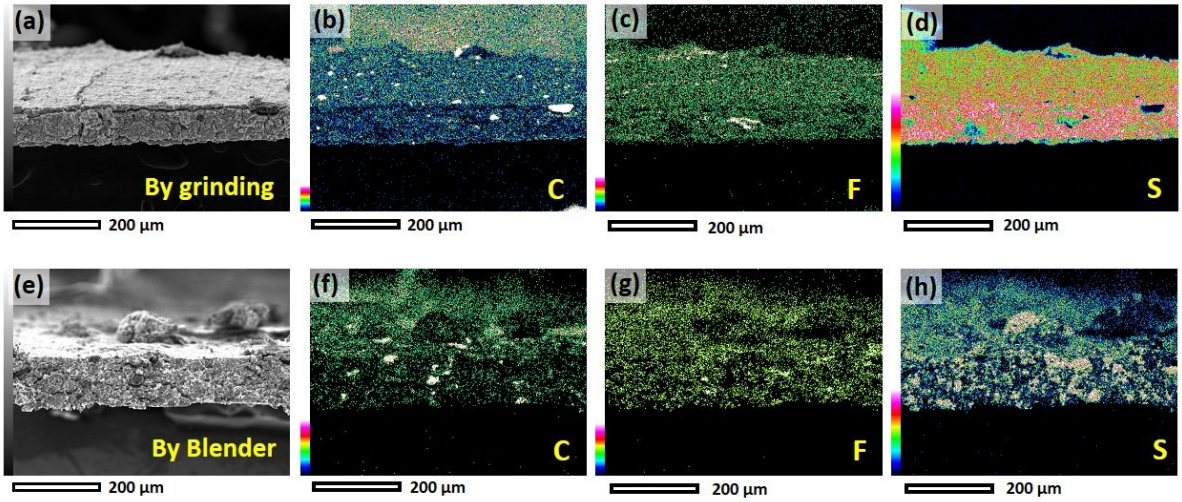

Figure 35. SEM images and EDAX mapping of C, F and S elements of (a-d) SSE composite film by grinding and pressing and (e-h) LCO cathode composite film by blending using a blender. Both films have the same formulation of "Active material/PTFE/Carbon 1/Carbon 2 = 94/3/1/2, wt%" though the active materials were different.

The above results proved that blending in a blender is a better process for large scale cathode and SSE film fabrication.

*31. **Ionic-conductivity stability of sulfide SSE in dry air**------- Li_2S-P_2S_5-P_2O_5-LiI (LPS-with LiI doping)*

The ionic conductivity and air stability are two key parameters that determine the performance of all solid-state batteries, therefore we listed them as our Go/No-Go milestones and made a lot of effort to improve them. Previously we have reported an LPS-P_2O_5-CaO solid electrolyte that barely met the 8-hour life requirement (77% ionic conductivity retention after 8 hours exposing to dry air), but the ionic conductivity was only ~0.5 mS/cm.

We further improved the ionic conductivity of air-stable SSE materials by LiI doping and tested its 8-hour stability in dry air. In brief, the Li_2S-P_2S_5-P_2O_5-LiI (LPS-LiI) solid electrolyte was prepared via a mechanical milling method as followed. A mixture of lithium sulfide (Li_2S, Sigma-Aldrich), phosphorus pentasulfide (P_2S_5, Sigma-Aldrich), phosphorus pentoxide (P_2O_5, Sigma-Aldrich) and lithium iodide (LiI, Sigma-Aldrich) was milled in a zirconia (ZrO_2) jar with the volume of 50 mL at a fixed rotation speed of 500 rpm for 40 h. The molar ratio is Li_2S: P_2S_5: P_2O_5: LiI = 75: 21: 4: 20. The synthesis was successfully scaled up to 50g/jar now using a large ball mill and 500mL zirconia jars and up to 200g/batch.

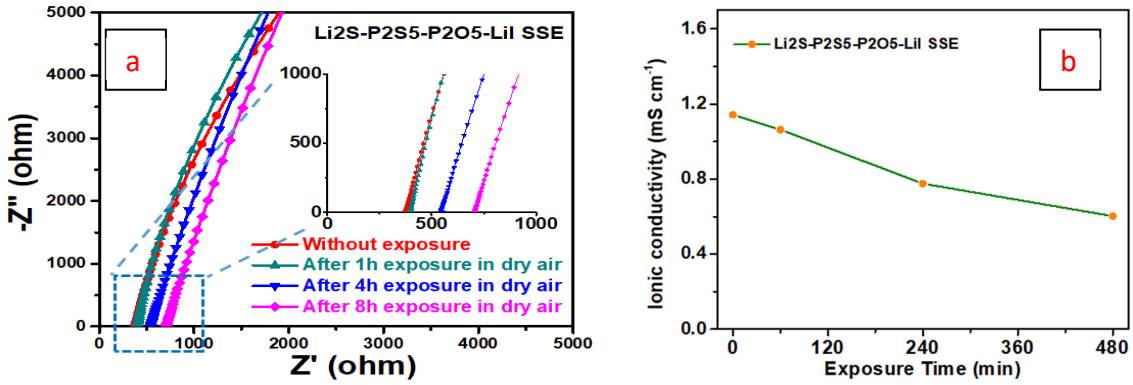

Figure 36. a) Impedance of the original Li_2S-P_2S_5-P_2O_5-LiI electrolyte and after exposure in dry air for 8 hours; b) Ionic conductivity change of the co-doped Li_2S-P_2S_5-P_2O_5-LiI electrolyte after exposure to the dry air up to 480 minutes.

As shown in **Figure 36a**, the bulk resistance of sulfide electrolyte pellet can be measured by EIS (0.1 Hz -1 MHz) and the ionic conductivity of electrolyte can be further calculated. From that bulk resistance (R), the ionic conductivity (σ) was calculated by using the equation $\sigma = d/(R \times A)$, where d was the thickness, and A was the area of the solid electrolyte pellet. As seen in **Figure 36b**, The initial ionic conductivity of the Li_2S-P_2S_5-P_2O_5-LiI electrolyte was measured to be 1.14 mS/cm. The value was slowly decreased by 6.7% and 32% after 1 hour and 4 hours exposure in dry air, respectively. Even after 8h exposure in air, the specific ionic conductivity still retained a high value of 0.60 mS/cm, which confirmed the long-time air-stability of **LPS-P_2O_5-LiI** solid electrolyte as well as its outstanding ionic conductivity.

32. SSB with various cathode materials-------s-NCM811 or s-NCM622 or s-LCO

In the last report, we had some initial results of SSB with surface coated NCM811 and NCM622 cathode materials, which showed a good first cycle capacity. As seen from **Figure 37**, the first cycle specific charge/discharge capacity and the Coulombic efficiency (CE) were 148/204 (mAh/g) and 73% for s-NCM811 SSB, 126/185 (mAh/g) and 68% for s-NCM622 SSB, 110/132 (mAh/g) and 84% for s-LCO SSB. The SSBs were disk-in-pouch cells with 10mm cathode/SSE/Li disk in a pouch. They were tested at 0.05C, 60 °C, at 3.0-4.3 V for NCM811 and NCM622, and 2.7-4.2V for LCO SSB. The reversible cell areal capacity was around 1 mAh/cm^2. The SSE used in those SSBs was LPS-glass-ceramic (LPS-GC) without

any additives for initial study. The cell performance is expected to be better by using either P_2O_5/CaO additives and P_2O_5/LiI additives later.

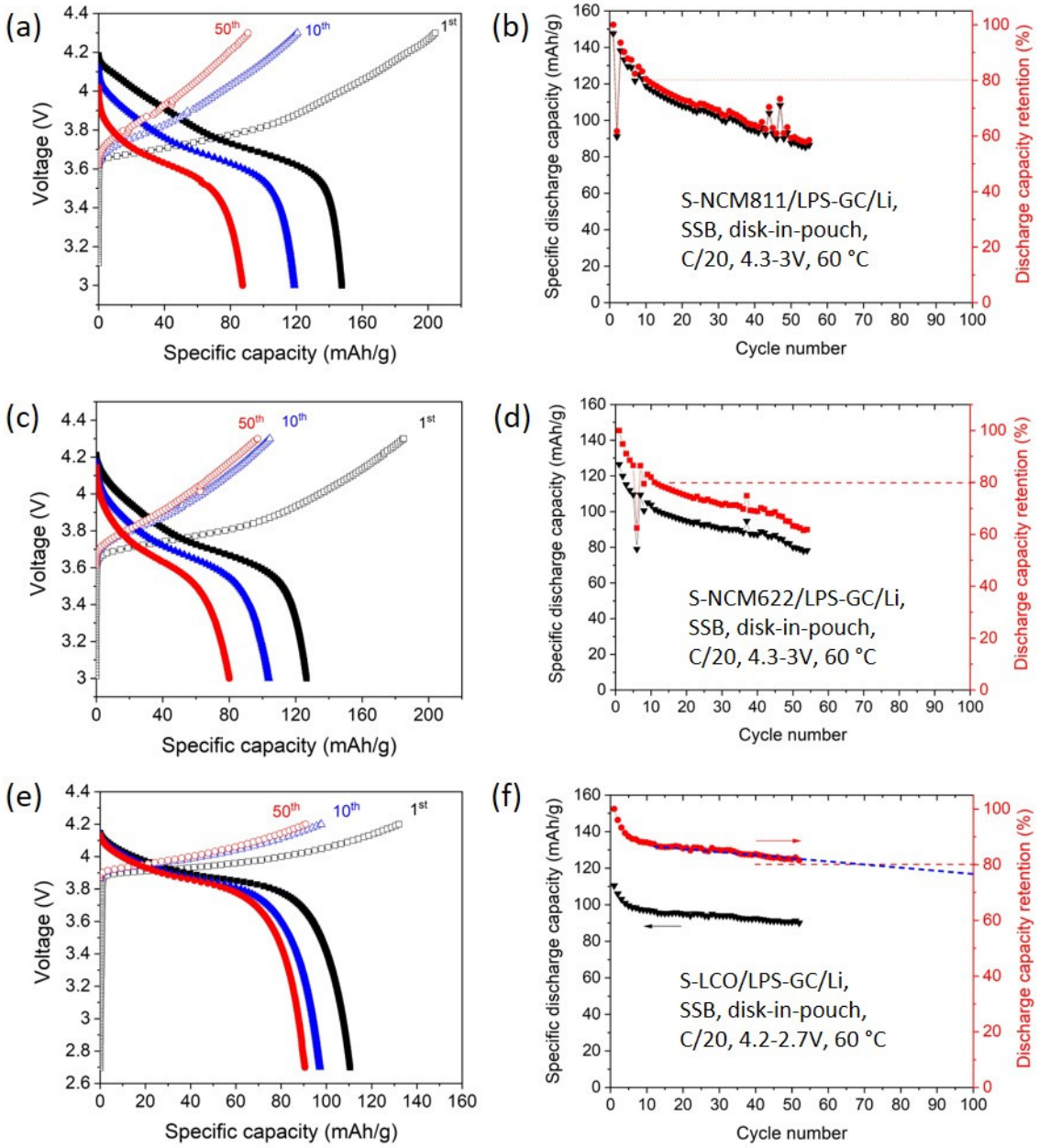

Figure 37. Charge-discharge profiles and cycle life results of the Cathode/LPS-GC/Li disk-type SSB with (a, b) surface-coated NCM811, (c, d) surface-coated NCM622, (e, f) surface-coated LCO cathode materials. The SSBs were disk-in-pouch cell with 10mm cathode/SSE/Li disk in a pouch. They were tested at 0.05C, 60 °C at 3.0 – 4.3 V for NCM811 and NCM622, and 2.7-4.2V for LCO SSB. The reversible cell areal capacity was around 1 mAh/cm².

With the application of the surface-coated NCM cathode and the improvement of the ionic conductivity of the LPS-glass-ceramic SSE, the SSBs with NCM811 and NCM622 started to output discharge capacity close to normal level, however the capacity still faded fast, showing only about 10 cycle life for both SSBs with NCM811 (**Figure 37b**) and NCM622 cathode (**Figure 37d**). In contract, the SSB with surface protected LCO cathode had much slower capacity fading, showing ~82% discharge capacity retention at

the 50th cycle, and was expected to show a cycle life of around 70 cycles (**Figure 37f**). It is worth pointing out that the specific discharge capacity of the SSB with s-NCM811 was higher than that with s-LCO before 50 cycles, and became same level of ~90mAh/g for both, meaning that for short-term cycling the SSB with s-NCM811 may have higher cell level capacity than that with s-LCO cathode. With this in mind, we were still majorly working on the most stable LCO cathode and will transfer the learning to NCM SSB later.

33. RT cell performance with LPS-LiI SSE*------disk-type cell s-LCO/LPS-LiI/Li*

Previously no SSB worked well at room temperature (RT) due to low ionic conductivity of the LPS SSE. Since we have developed the LPS-LiI SSE with much higher RT ionic conductivity of 1.14 mS/cm, we tried again on the RT cell performance test on a s-LCO/LPS-LiI/Li disk-pouch cell. The cell was first cycled at 60 °C for 1 cycle and then cycle at RT at 0.05C. The first cycle voltage profiles at both temperatures were shown in **Figure 38**.

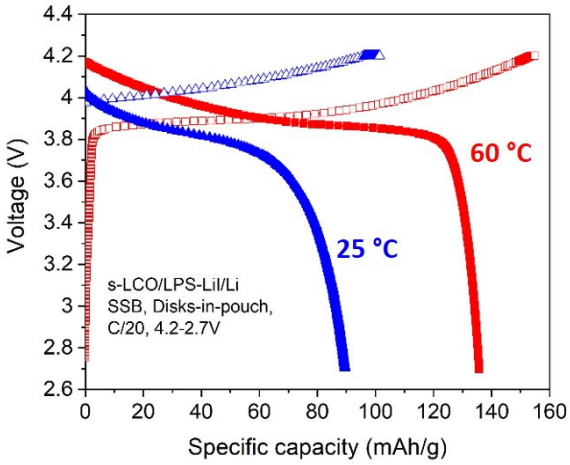

Figure 38. Charge-discharge profiles of a s-LCO/LPS-LiI/Li SSB at 1st cycle at 60 °C and the following cycle at RT. The SSBs are disk-in-pouch cell with a 10mm cathode/SSE/Li disk in a pouch. It was tested at 0.05C, 2.7 – 4.2 V. The reversible cell areal capacity was around 1 mAh/cm².

Due to the much higher ionic conductivity of the LPS-LiI SSE, the specific discharge capacity was increased to up to 136 mAh/g at 60 °C (about 10 mAh/g higher than using LPS-GC). The specific discharge capacity at RT was about 90 mAh/g, not very high but much better than before.

34. Preliminary test cells*------5 disks in each pouch cell*

The pouch cell assembling procedure has been demonstrated in a 3.5x5 cm size pouch cell. Cell chemistry has been demonstrated but the formulation and processing of the cathode and SSE composite need to optimize for a better balance of cell performance and film strength for R2R process. Due to the previous instrument repairing of ball mill and heated roll press, we adopted the multiple 10mm size disks (5 disks in each pouch cell for this 12 preliminary cells) of s-LCO/LPS-LiI/Li enclosed in a pouch for these preliminary test cells, which can perfectly simulate the pouch cell performance. We are currently working on the R2R process for the large area cathode and SSE film.

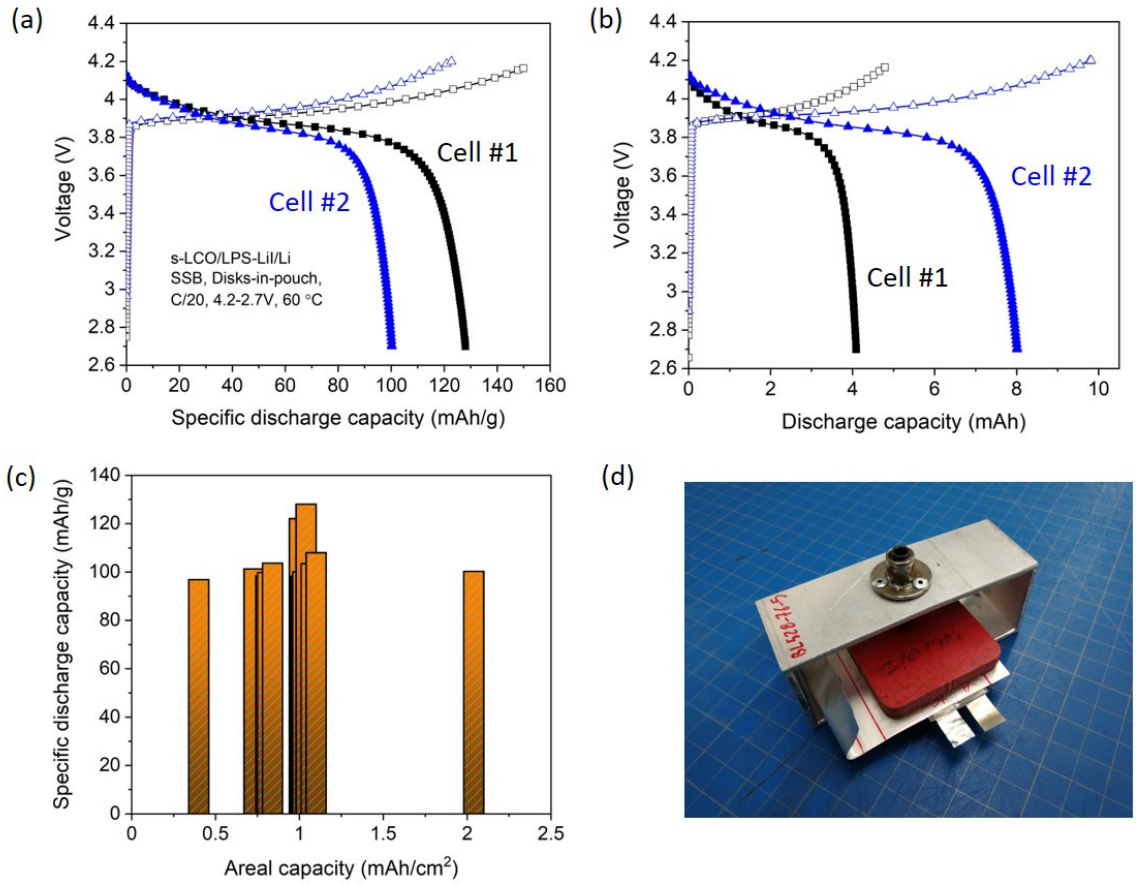

Figure 39. Performance of s-LCO/LPS-LiI/Li solid-state batteries to be delivered to DOE. (a) Specific discharge capacity and (b) cell discharge capacity of two typical SSB with 4 mAh and 8 mAh reversible discharge capacity. (c) Statistical information of the cell specific discharge capacity and areal capacity in the first cycle. (d) A photo of a pouch solid-state battery. The SSBs are disk-in-pouch cell with multiple 10mm disks in a pouch. They were tested at 0.05 C, 60 °C at 2.7-4.2V.

The cell performance and information were shown in **Figure 39**. All the cells were completed one formation cycle at 0.1C charge/discharge rate, 2.7-4.2V at 60 °C. Most of the cells have a reversible cell capacity of 4mAh and we have designed a few cells with higher capacity of 8mAh or lower capacity of 2mAh to cover a wider range. A typical s-LCO/LPS-LiI/Li SSB cell has a ~1 mAh/cm^2 areal capacity and 4mAh cell capacity, showing ~100 mAh/g and up to 128 mAh/g specific discharge capacity.

We used cell #3 for a further test of high-rate cycling. It may be worth to point out that performance of Cell #3 during formation was a little low, so a normal cell should have a better performance. The first specific discharge capacity of Cell #3 was 93 mAh/g when cycling at 0.1C charge/discharge rate. It dropped by 33% to 62 mAh/g. The cycle life of Cell #3 was about 16 cycles at C/3 discharge rate as shown in **Figure 40**.

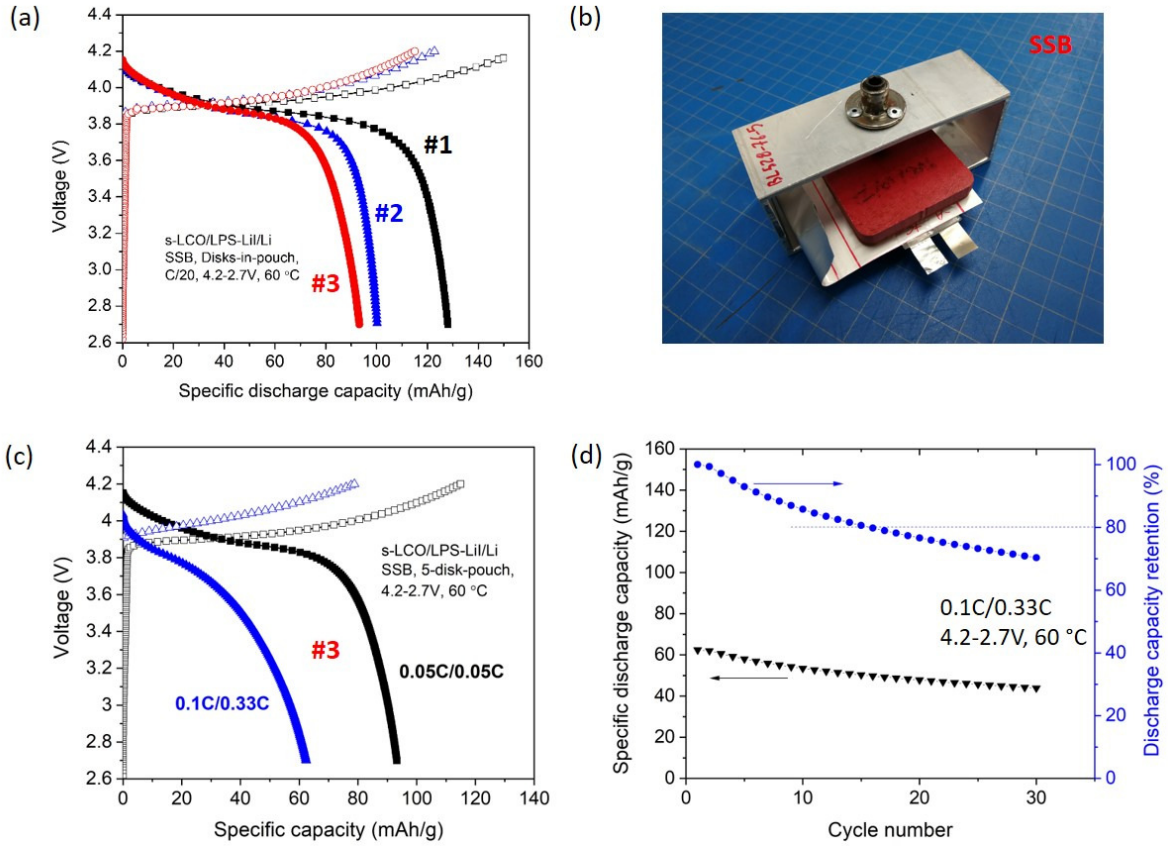

Figure 40. Performance of s-LCO/LPS-LiI/Li solid-state batteries. (a) Specific discharge capacity and (b) A photo of a pouch solid-state battery. (c) Cell #3 charged and discharged at higher rate vs low rate during formation. (d) The cycle life of Cell #3 at high rate of 0.1C charge and 0.33C discharge vs at low rate during formation, 60 °C at 2.7-4.2V. The SSBs are disk-in-pouch cell with multiple 10mm disks in a pouch.

35. Dry process cathode and SSE development------New PTFE binder and New Carbon additives

Our target process will use R2R processed cathode and SSE film for the 2.5Ah solid-state batteries, but due to the addition of non-active components of polymer binder and additives that is necessary to make the film flexible and robust, as well as different processing procedure, the SSB cells did not work well when we use these R2R processed cathode and SSE film. We are trying to solve the issue because this becomes the major barrier. Two strategies were adopted: (1) optimizing by using new materials, (2) optimize the processing procedure. Most recently, we made some progress on the former strategy introducing new PTFE binder and conductive carbon additives.

As shown in **Figure 41a**, the black line represented the resistance of current cathode film. When we use a new PTFE polymer binder (red line), the resistance reduced significantly. In a new series test using this new PTFE binder (**Figure 41b**), two new conductive carbon additives were used. When the conductive carbon additive (CC2) was used, the resistance of cathode film increased, but when new carbon additive CC1 was used, the film resistance decreased to a very low level. We expect this change may boost the cell performance.

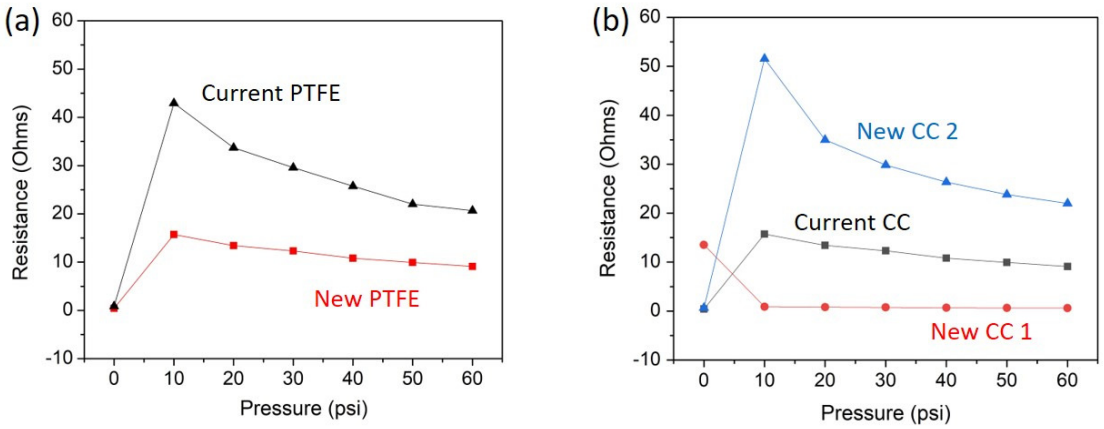

Figure 41. (a) Resistance of the dry processed NMC622 cathode film using different PTFE polymer binders. (b) Resistance of the dry processed NMC622 cathode film using different conductive carbon additives.

36. R2R SSB cathode and SSE film development

Distinct with other film fabrication for solid-state batteries, the solvent-free cathode and SSE film processing shows its unique advantages (e.g., low cost, mild condition, environment friendly, less side reactions, thick cathode fabrication, etc.). So far, most solvent-free electrode and SSE film processing is limited in lab scale by hydraulic pressing, which prevent its application in industries. Because PVDF binder is not able to fibrillate in dry form, PTFE is used as binder in dry film processing. However, without the solvent to disperse the polymer binder as that in normal PVDF/NMP system, the efficiency of PTFE binder fibrillization is typically low. In addition, the adhesion of PTFE is weaker than PVDF. These cause a high content of PTFE binder usage, which consequently reduces the active material content and low conductivity of the film. It has more obvious negative effect on the ionic conductivity of SSE film. We have tested using of new PTFE binder and new carbon additives to increase the tensile strength of NMC622 cathode film from 0.71 N/mm^2 (sample 1 in Table 1) of baseline to 1.65 N/mm^2 (sample 2 in **Table 3**). In last quarter, we developed a new carbon additive, CC 2 for cathode with much lower cost but comparable tensile strength of 1.20 N/mm^2 (sample 3 in Table 1) to replace the more expensive CC 1.

Table 3. Mechanical performance of NMC622 cathode film with various new components and processing technology.

Sample	Force @ Peak (N)	Young's Modulus (N/mm^2)	Tensile Strength (N/mm^2)
(1) PTFE 0, CC 0, std	1.64	306.04	0.71
(2) PTFE 1, CC 1, std	4.17	714.38	1.65
(3) PTFE 1, CC 2, std	2.92	244.60	1.20
(4) PTFE 1, CC 2, Adv	7.25	1455.54	**3.07**

Note: CC 0 and PTFE 0 are baseline carbon additive and polymer binder. CC 1 and CC 2 are new carbon additives. PTFE 1 is new polymer binder. Std stands for standard dry processing. Adv stands for advanced dry processing. 5 wt% PTFE binder was used in all these samples.

The above development was based on Navitas' standard dry processing procedure. Navitas has initiated an advanced dry processing technology in the first year of Phase II under Battery 500 seeding project. In the most recent test of cathode film fabrication, the tensile strength of NMC622 cathode film showed ~250% increase to 3.07 N/mm^2 (sample 4 in Table 1). This is a significant progress on the dry film processing. Previously we have suffered from either low film strength when using less PTFE binder or low conductivity when using higher PTFE binder, which is a big barrier that prevents us to fabricate cathode and SSE film that has a good balance between mechanical properties and electrochemical properties. In our standard dry processing, we have to use at least 9 wt% of PTFE binder to make the film which has reasonable strength to handle during film calendaring and cell assembly, but at such high binder content, the conductivity of the film was too low to make the SSBs work normally. These new films also showed a relatively good flexibility as shown in **Figure 42**.

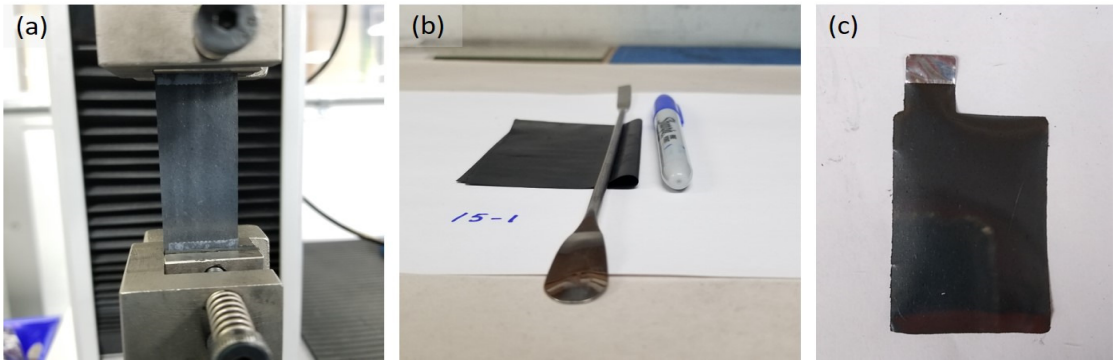

Figure 42. Quality control of the solvent-free processed NMC622 cathode films. (a) Tensile strength test. (b) Flexibility test. (c) A laminated NMC622 cathode on Al foil for pouch cells. 5 wt% PTFE binder was used in these films.

This new advanced solvent-free mixing technology paves a way for a low binder content cathode and SSE film due to high efficiency of fibrillating PTFE binder. We believe that the usage of this technology towards solvent-free processing of solid-state cathode and electrolyte film will make the unique and promising technology more practical.

*37. **Solid-state cell material and configuration development**------ Li_6PS_5Cl (LPSCl)*

We have developed a LiI-doped sulfide electrolyte (LPSI) with high ionic conductivity >1.1 mS/cm (**Figure 43b**) and are using it in SSE film. However, it may have side reactions with lithium metal and cause a fast degradation and short cell life. Therefore, we have tested a new but same argyrodite-type solid electrolyte Li_6PS_5Cl (LPSCl), which should have similar ionic conductivity but higher stability.

Our subcontractor, UMD Prof. Wang's group has demonstrated the synthesis in small scale and the ionic conductivity of 1.1 mS/cm (**Figure 43a**), which is same with the LPSI. Navitas is currently scaling up the ball mill synthesis of LPSCl using the same procedure for LPSI.

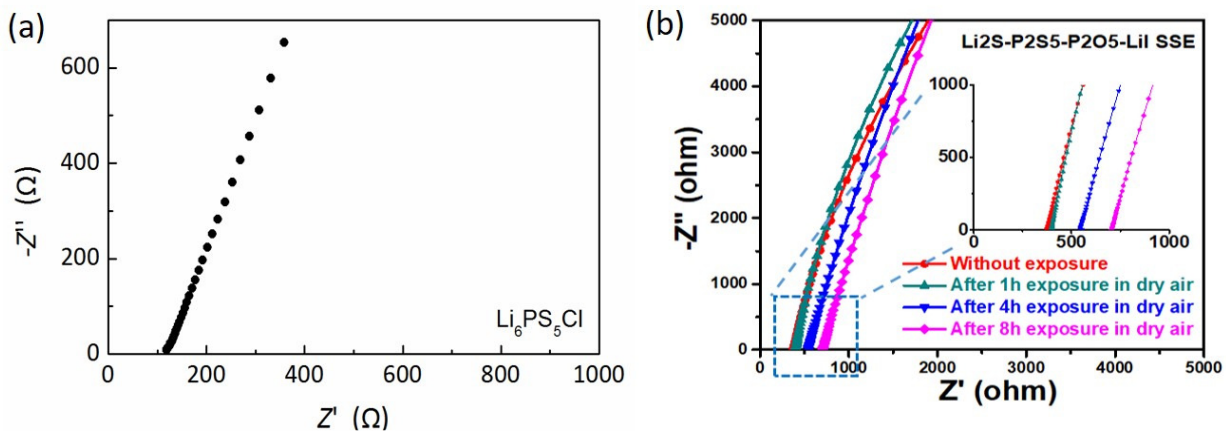

Figure 43. (a) Impedance of the annealed LPSCl electrolyte. (b) Impedance of the LPSI electrolyte before and after exposure in dry air for up to 8 hours.

38. ***Disk-type Solid-State Cell Performance*****------** *double layer SSE with LPS and Li_6PS_5Cl (LPSCl)*

Although the LPSCl electrolyte should be more stable than LPSI we used, it may still have relatively fast decay while contacting bare lithium anode. Considering the glass ceramic LPS (LPS-GC) has the best stability among them, we have tested the published concept by using double layer SSE with LPSCl as major component and a thin layer of LPS-GC facing lithium metal anode. As seen in **Figure 44a**, the SSB of LCO/LPSCl/Li pouch cell showed the first specific discharge capacity of 76 mAh/g when cycling at C/10 rate at 60 ˚C, while the SSB using double layer SSE exhibited much higher specific discharge capacity of 98 mAh/g. The LPSCl solid electrolyte we used in these cells had very long storage time and caused the low specific capacity, but the results clearly demonstrated the double layer SSE has much better cell performance.

As shown in **Figure 44b**, the SSB using double layer SSE film had higher capacity and longer cycle life than the SSB with single layer LPSCl SSE, though the cell capacity decay rate is still in high range, which might be caused by serious side reaction with lithium and should be able to improve by lithium metal protection.

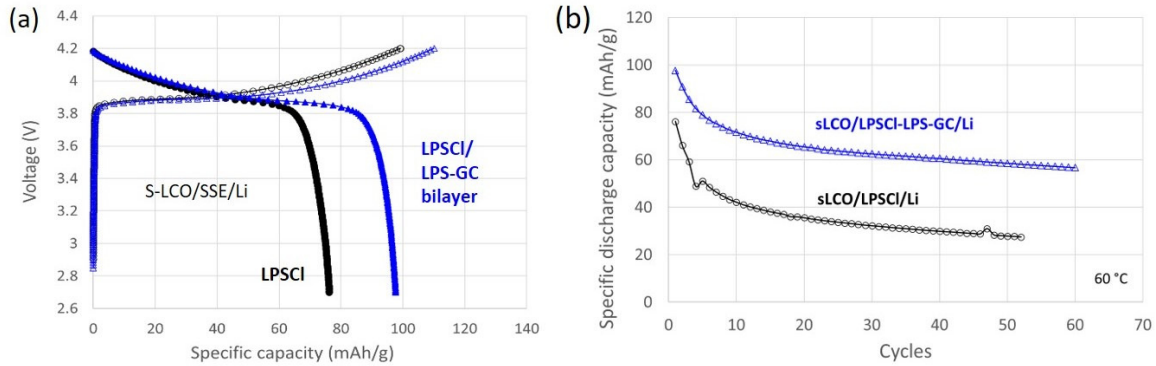

Figure 44. Performance of s-LCO/SSEl/Li solid-state batteries. (a) Specific discharge capacity and (b) the cycle life of SSB with single layer LPSCl (black) or double layer LPSCl/LPS-GC SSE film (blue) of pouch cells cycling at 0.1C charge and discharge rate, 60 °C and 2.7-4.2V. The SSBs are disk-in-pouch cell with 10mm disks in a pouch.

*39. **Solid-state cell assembly and test**------disk-type s-LCO/LPS/Li cells under various pressure*

In the early stage of the SSB development, we have a brief screening of the cell pressure effect on SSB cell capacity. We were able to locate the best range for high cell performance between 2-4 psi (**Figure 45a**). Recently, we detailed the cell pressure range of 2-4 psi, and the results showed the highest cell capacity at 2.6 psi **(Figure 45b)**, with the first specific discharge capacity of 94 mAh/g, 116 mAh/g, 97 mAh/g for cell pressure of 2.2 psi, 2.6 psi and 3.5 psi, respectively.

Considering most of our SSB were using 2.2 psi pressure in our previous studies, the cell capacity maybe improved by using the higher pressure of 2.6 psi. The SSB cycle life is possible to be improved since the deposition of lithium will be much dense under higher pressure.

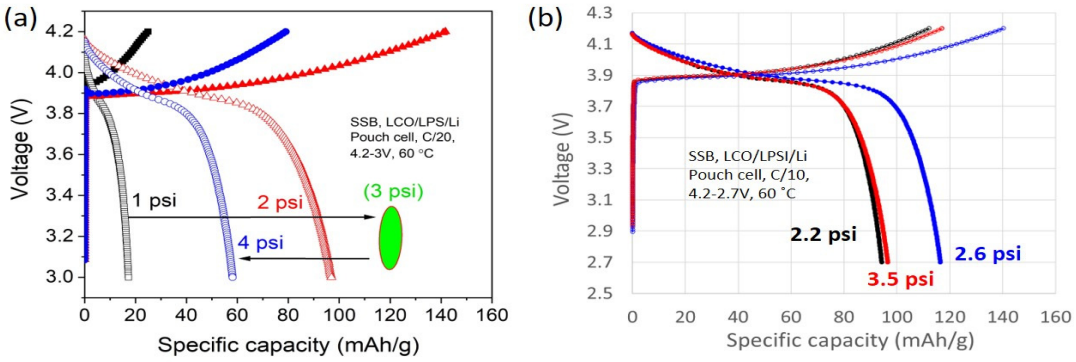

Figure 45. Performance of s-LCO/LPS/Li solid-state batteries under various pressure. (a) Previous results from LCO/LPS-GC/Li pouch cells cycled at C/20, 4.2-3V, 60 °C. (b) Recent results from LCO/LPSI/Li pouch cells cycled at C/10, 4.2-2.7V, 60 °C. The SSBs are disk-in-pouch cell with multiple 10mm disks in a pouch.

Phase II: No-Cost Extension

*36. **Solid-state electrolyte composite film and single layer pouch cell**------LPSCl SSE*

Synthesis of LPSCl with LiCl precursor having smaller particle size

It has been well known that particle size of solid-state electrolyte plays an important role in solid-state battery. We have prepared the LPSCl by ball milling Li_2S and P_2S_5, and LiCl precursor was sieved with 20 µm size sieves. The ball milled Li_2S and P_2S_5 samples were mixed/ground with the sieved LiCl, then annealed at 500 °C for 4 hours. As it can be observed in **Figure 46a**, LPSCl prepared in this way has an irregular shape, with particle size smaller than 20 µm **(Figure 46b)**. The XRD showed the LPSCl argyrodite structure is cubic with space group F-43m **(Figure 46c)**.

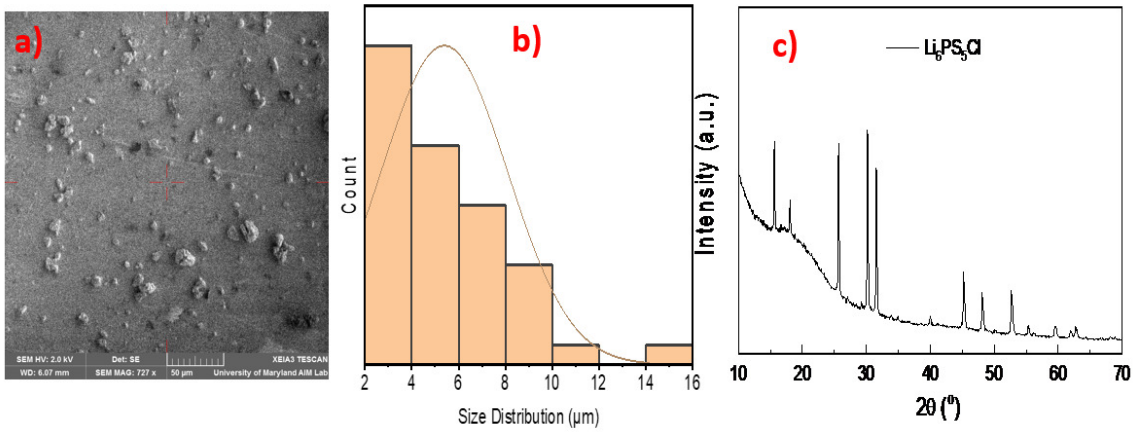

Figure 46. The LPSCl prepared by ball milling Li_2S, P_2S_5, and LiCl was sieved through 20 μm sieves before solid-state reaction at 500 °C: a) SEM image; b) Particle size distribution; and c) XRD of LPSCL.

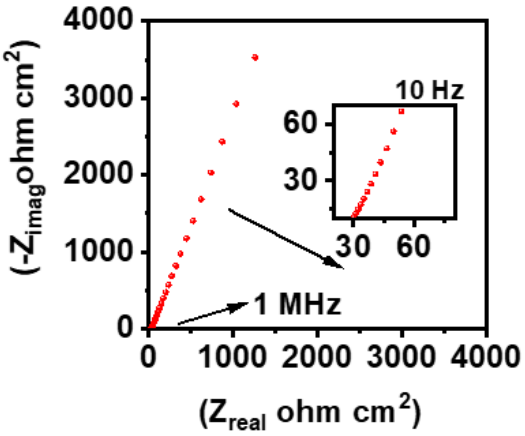

Figure 47. Ionic conductivity values of the LPSCl prepared by **ball** milling Li_2S, P_2S_5**,** and LiCl was sieved through 20 μm sieves. Solid-state reaction at 500 °C for 4 h.

Ionic conductivity measurement showed LPSCl has a high value of 3.3 mS/cm (**Figure 47**), which is suitable the solid-state battery application. The solid-state electrolyte LPSCl synthesized in this way will be used for the whole no-cost-extension period.

We developed a process that enables us to produce large size (> 12 cm^2) free-standing and flexible SSE (**Figure 48a)** to assemble and test the single layer pouch cells. The initial thickness of the as prepared SSE film (mixture of 99.6% LPSCl and 0.4 wt% PTFE) is around 220 μm **(Figure 48b**). The thickness of the SSE film can be further reduced to less than 80 μm. However, handling such thin films becomes a challenge as it starts to break during handing. Therefore, for the optimization of initial cell assembly process and to tune the stacking parameters we have kept the SSE thickness over 200 microns. Next, the cathode powders (mixture of 70 wt% NMC811, 28% LPSCl and 2 wt% CNT) were added on top of SSE film and pressed under a hydraulic press, after which the stack was vacuum sealed in the pouch materials to prepare a single layer pouch cell (**Figure 48c**). The active area in this cell is about 4 cm^2. The total cathode loading has been about 4 mg/cm^2. The initial electrochemical performance of the SLP is presented in **Figure 48d**. The first cycle discharge capacity was about 50 mAh/g while the first

cycle efficiency was 44%. In our cold-pressed disc type cells, we could achieve as high as 160 mAh/g with the same cathode and SSE combinations. We believe the cell stacking pressure used to laminate cathode to the SSE layer needs to be further optimized to unlock more capacity from the existing setup. Currently, we are examining the role of different laminating pressures used to prepare the stack to evaluate the capacity delivery in the SLPs.

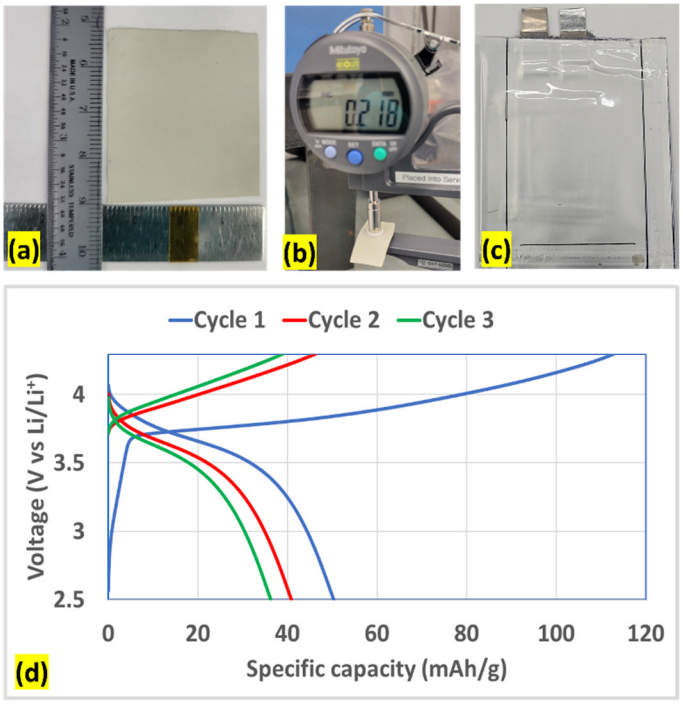

Figure 48. Preparation and testing of single layer pouch cell (SLP). (a) Free standing and flexible solid-state electrolyte (SSE) containing 99.6% LPSCl and 0.4 wt.% PTFE, (b) initial thickness ~218 microns, (c) vacuum sealed SLP, (d) electrochemical performance of the SLP presented for first 3 cycles. The cell was tested at 60°C at the current density of 0.1 C (1 C = 160 mA/g) between the voltage range of 2.5 to 4.3 V.

42. SSB cathode development------Al_2O_3-coated NMC811 (s-NMC811) cathode powder

It has been observed that cobalt containing cathode materials without any protective surface-coating undergo rapid capacity fade when cycled with sulfide-based electrolyte. We have tried polycrystalline NMC811 from several vendors, a sample of single crystal NMC811 as well as polycrystalline NMC811. A common behavior among all those materials was that the capacity retention of such cathodes were less than 10 cycles for 80% retention. We also evaluated NMC811 cathode with $LiNbO_3$ surface coating. However, no significant improvement on cycle life or specific capacity was observed. Recently, we partnered with a domestic electrode materials coating company, which provided us the cathode materials with Al_2O_3 coated on the electrode surface. The electrochemical performance of the baseline NMC811cathode as well as the three samples with different thicknesses of Al_2O_3 coatings are presented in **Figure 49**.

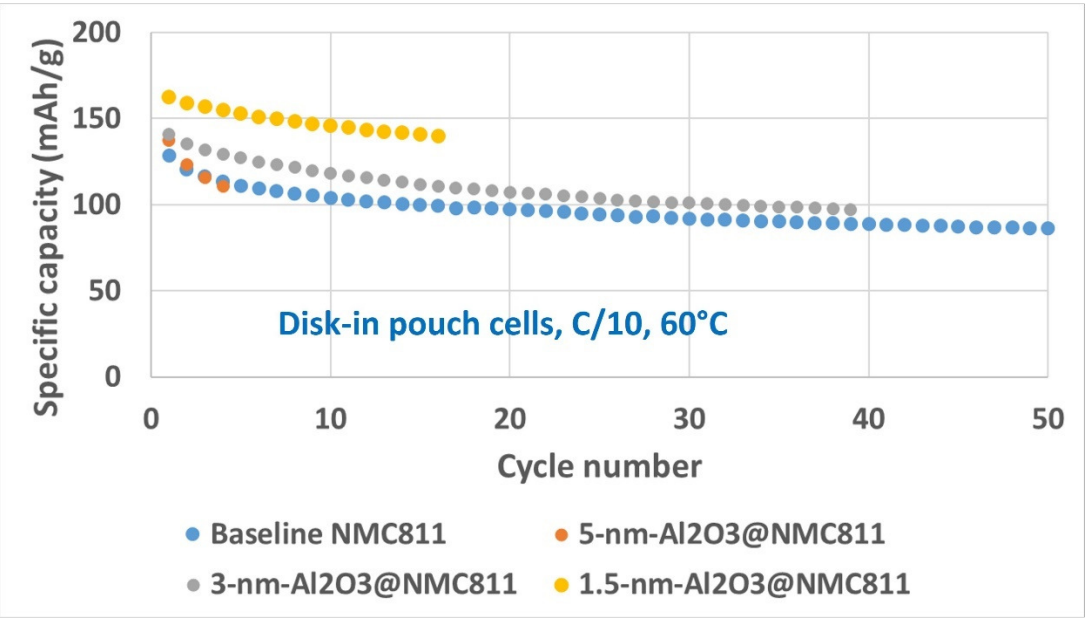

***Figure 49**. Comparison of electrochemical performance of baseline NMC811 cathode and the same cathode coated with Al_2O_3 of different thicknesses (i.e., 1.5 nm, 3 nm, and 5 nm). The cells were tested at 60°C at the current density of 0.1 C (1 C = 160 mA/g) between the voltage range of 2.5 to 4.3 V.*

The baseline NMC811 offered the initial discharge capacity of 129 mAh/g with FCE 66.7%. The capacity fade was rapid for the first few cycles, losing about 20% of its initial discharge capacity in just 11 cycles. Later, however, the capacity started to level off. After 39 cycles, the capacity retention was about 70%. The cathode sample coated with 5 nm Al_2O_3, lost more than 20% in just four cycles. However, the sample with 3 nm Al_2O_3 not only offered higher initial discharge capacity, but also retained 80% after 15 cycles. The best performance in terms of initial discharge capacity and cycle life for 80% retention was offered by the sample with 1.5 nm thick coating of Al_2O_3. The initial discharge capacity was ~162 mAh/g with FCE about 78%. The capacity retention after 16 cycles was 86%. These results suggest enhanced electrochemical performance of the NMC811 cathode enabled by thin layer of Al_2O_3 coating.

*43. **Li metal protection------** LPO (Li_3PO_4) coated Li metal*

We have recently received first batch of LPO (Li_3PO_4) coated Li metal anode from Oak Ridge National Laboratory (ORNL). The thickness of the coating was about 0.5 to 1 micron.

As seen in **Figure 50a**, darker surface on top of the free-standing lithium foil is the LPO coated side. The bare/back side of the foil is presented in **Figure 50b**. The total thickness of the foil with coating is about 53 microns (**Figure 50c**). The thickness of the coating itself is about 0.5 to 1 micron. The electrochemical performance of all solid-state cells with LPSCl as SSE and $LiNbO_3$ coated NMC811, with and without LPO coated Li anode are compared in **Figure 50d**. The baseline cell with bare Li foil offered the initial discharge capacity of 129 mAh/g whereas LPO coated anode led to lower capacity of 97 mAh/g. Even though the initial charge capacity of both cells is very similar (~187 mAh/g), the LPO coated anode resulted in much lower coulombic efficiency (~51%) compared to the baseline cell that delivered 69%. We repeated the similar cells with LCO cathode as well and the results suggested similar behavior in terms of capacity as cycle life. Furthermore, none of the cells with LPO anode achieved more than 2 cycles. These results

suggest the thin layer of LPO may not provide a reliable protection to Li anode thereby fails at preventing internal shorting and minimizing the irreversible capacity loss.

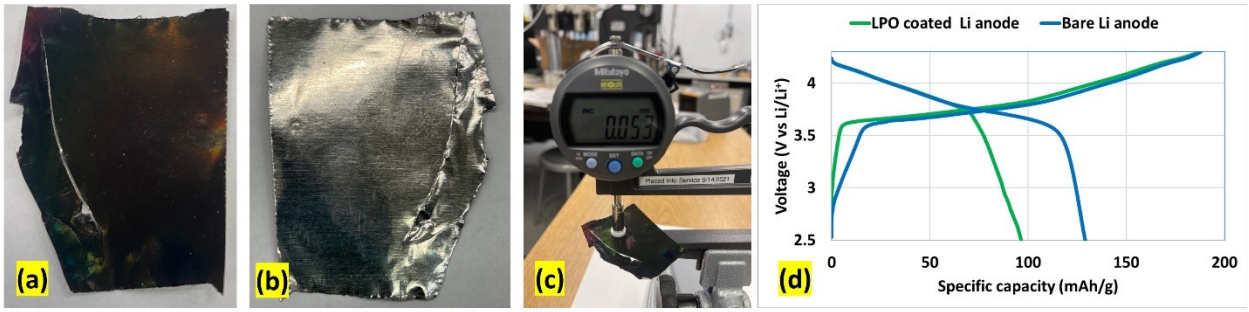

***Figure 50**. LPO coated Li metal foil and evaluation of electrochemical performance. (a). The LPO coated surface on top of Lithium foil, (b). bare back side of the Li foil, (c) thickness measurement suggesting the total thickness around 53 microns (d) first cycle charge and discharge capacity comparison between bare and LPO coated Li foil anode with LPSCl based SSE and NMC811 cathode. The cells were tested at 60°C at the current density of 0.1 C (1 C = 160 mA/g) between the voltage range of 2.5 to 4.3 V*

44. Evaluation of 1.5 nm Al_2O_3-coated NMC811 (s-NMC811) cathode powder

The electrochemical performance of 1.5 nm Al_2O_3 coated NMC811 cathode is presented in **Figure 51**. After 20 cycles, the specific capacity of NMC811 is still around ~ 140 mAh/g (more than 80% capacity retention). The specific capacity decreased with the increase in cycle number, but it still maintained ~ 106 mAh/g after more than 100 cycles, indicating that 1.5 nm Al_2O_3-coating onto NMC811 improved the cycle life of ASSB.

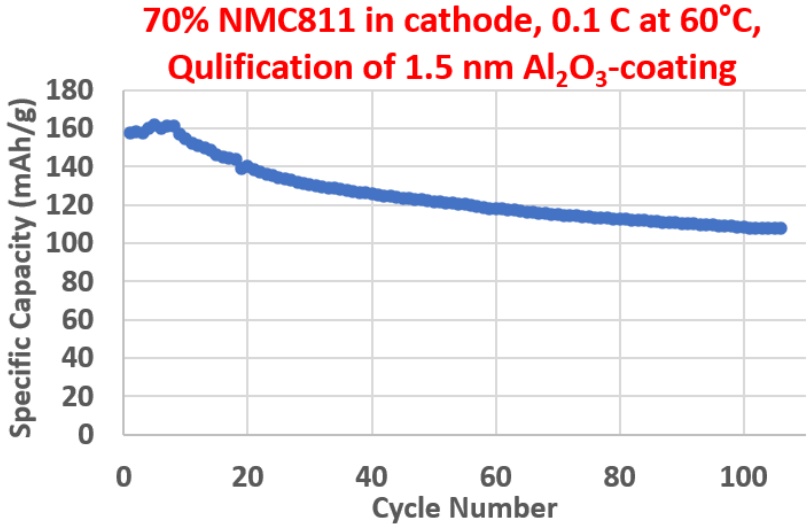

***Figure 51**. Electrochemical performance of NMC811 cathode coated with Al_2O_3 (1.5 nm). The disk-in pouch cell was tested at 60°C at the current density of 0.1 C (1 C = 160 mAh/g) between the voltage range of 2.5 to 4.3 V. Cathode loading: ~ 0.784 mAh/cm^2.*

45. The minimum requirement of PTFE% to make free-standing s-NMC811 cathode films

For free-standing solid-state electrodes, the binder will dramatically influence the cell performance because, contrary to liquid electrolyte systems, the binder can actively block the surface of the active material and cut conduction pathways. Nevertheless, the binder is an inactive material in the cathode composite lowering the over-all cathode density. To make a free-standing cathode film and all-solid-state battery scalable, binder is a must in cathode. Therefore, the aim of this study was to decrease the PTFE binder amount to an absolute minimum when a free-standing cathode film can be fabricated. In previous reports, the free-standing SSE films contain 0.4 wt% PTFE; For the cathode composite, less than 0.4% PTFE binder in cathode is a good starting point. **Table 4** summarized the testing results of PTFE% requirement to make a free-standing cathode film. It was found that 0.1% and 0.2% PTFE in cathode composites are not enough to make a free-standing cathode film. 0.3% PTFE is good enough to binder s-NMC811, CNT, and SSE together and make a free-standing cathode film. It must be mentioned, 0.3% PTFE may not be an optimized number.

Table 4. *Design of experiment to make a free-standing cathode film with minimum PTFE%.*

Sample #	s-NMC811 (%)	SSE (%)	CNT (%)	PTFE (%)	Notes
1	**69.9**	**28**	**2**	**0.1**	**Can't make free standing cathode film**
2	**69.8**	**28**	**2**	**0.2**	**Can't make free standing cathode film**
3	**69.7**	**28**	**2**	**0.3**	**Can make free standing cathode film!**

Therefore, SLP/DLP pouch cells can be assembled with freestanding cathode and SSE films, which could be scaled up for future study.

46. Performance of disk-pouch cell with 0.3% PTFE binder in s-NMC811 cathode

In all previously tested disk-pouch cells, both cathode and SSE did not contain any PTFE. Therefore, it is worth investigating the effect of PTFE in both cathode and SSE to disk-pouch cell performance.

Figure 52 showed the disk-pouch cell performance with 0.4% PTFE in SSE, and 0.3% PTFE in s-NMC811cathode, respectively. It was found that the performance of disk-pouch cell with PTFE binder is comparable to that without PTFE, with a specific capacity of 155-160 mAh/g for s-NMC811, indicating that introducing PTFE in both cathode and SSE didn't affect the cell performance. Therefore, it is worth trying to make and test SLP and DLP cells with free-standing SSE and cathode films, which are necessary to fabricate multilayer cell stacks.

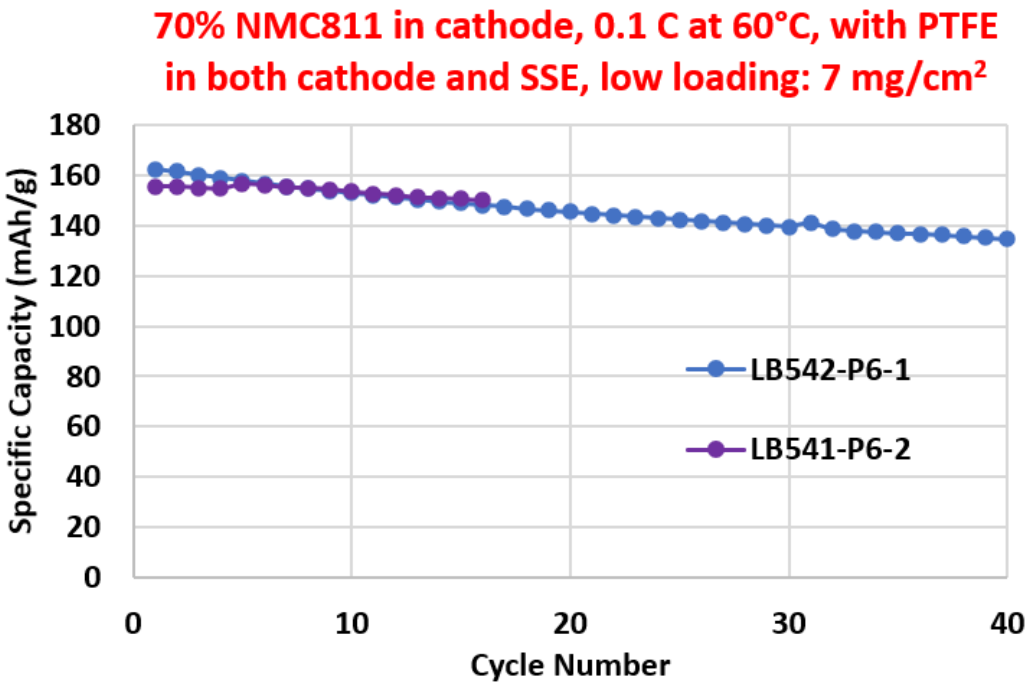

Figure 52. *Electrochemical performance of disk pouch Li/LPSCl-PTFE/NMC811-PTFE cell with PTFE in both cathode (69.7% of 1.5 nm Al_2O_3-NMC811 +28% SSE + 2% CNT +0.3%PTFE) and SSE (99.6% LiPSCl + 0.4% PTFE), areal capacity 0.78 mAh/cm^2. The cells were tested at 60°C and the current density of 0.1 C. (1 C = 160 mAh/g) between the voltage range of 2.5 to 4.3 V.*

47. Evaluate the SLP cells with Free-Standing 1.5 nm-Al_2O_3 coated NMC811 cathode film with low percentage of PTFE binder

we demonstrated our SLP preparation process: The powder mixture (NMC811 + SSE + CNT) was pressed against SSE to form cathode. In that case, it is exceedingly difficult to scale up the production of cathode and batteries. On the other hand, the powder cannot be distributed evenly, which causes trouble to reproduce the cell performance. In this report, we successfully demonstrated that cathode can be made as a free-standing film and incorporated into the All-Solid-State Battery. **Figure 53a** and **53b** showed our improved SLP process with free-standing cathode films which contains 0.3 wt% PTFE, the areal loading is ~ 7 mg/cm^2, size is 2 cm × 2 cm, and thickness is ~ 70 µm. It must be noted, we can control the thickness and areal loading easily through rolling-calendering process; And the free-standing cathode film can be made to a much larger film. The size of SSE is ~ 2.5 cm × 2.5 cm. The *Prime-coated* Al current collector, free-standing NMC811 film, and free-standing SSE films were laminated together at 120 °C, which would reduce the interface resistance.

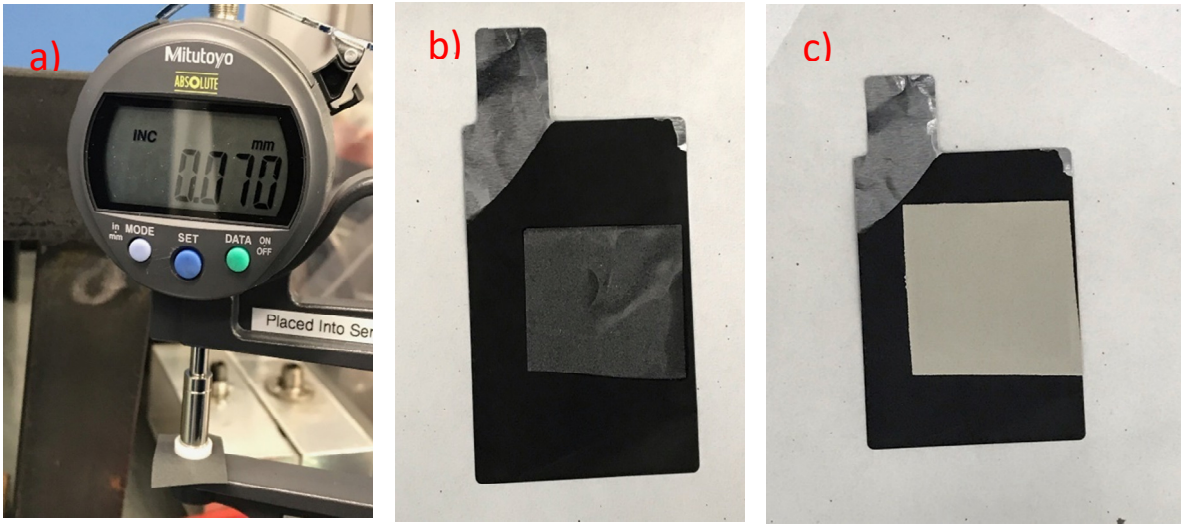

Figure 53. *a) thick ness Free-standing 1.5 nm-Al_2O_3-coated NMC811 electrode (2 × 2 cm, 69.7% NMC811+ 28% SSE + 2% CNT + 0.3% PTFE); b) Free-standing cathode film on carbon-paint-coated Al current collector; c) Prime-coated Al current collector, free-standing NMC811 film, and free-standing SSE film (2.5 cm × 2.5 cm, 99.6% SSE + 0.4% PTFE) were laminated together at 120 °C.*

We have investigated the effect of pressing pressure on the performance of cells, it seems that 6 tons are the best press pressure to assemble the all-solid-state-battery with Li anode, free-standing SSE, and free-standing cathode.

There are many factors to affect the specific capacity of NMC811, one of the most important factors is internal resistance of the ASSB. In all these factors, interface resistance plays a dominating role in the internal resistance in ASSB. To reduce the interface resistance between free-standing cathode film and prime-coated Al current collector, a thin layer of conductive carbon paint (**838AR from MG Chemicals**) was applied. **Figure 54** showed the performance of SLP (Cell stack **Fig. 53c** was pressed under 6 tons), the specific capacity of NMC811 is ~ 192 mAh/g. So far, it is the best SLP cell which delivered the expected specific capacity (220 ± 10 mAh/g in traditional NMC811 LIBs with liquid electrolyte). By improving the SLP assembling process, the higher specific capacity of NMC811 was successfully unlocked.

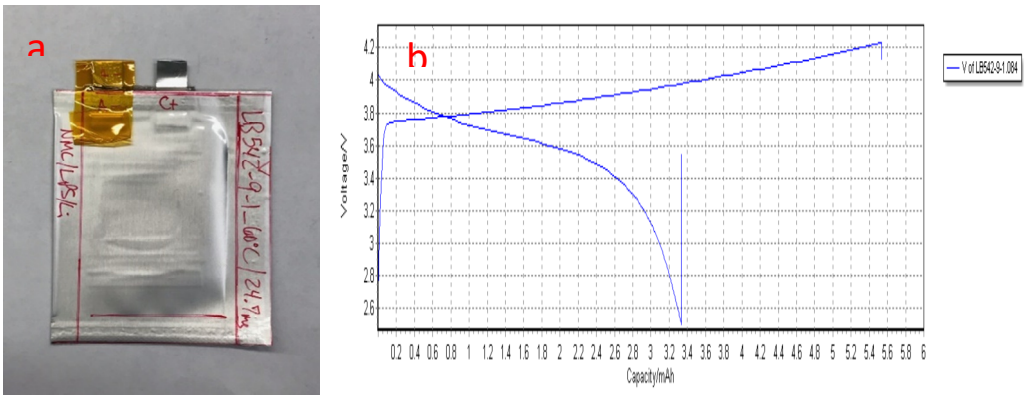

Figure 54*. (a) Picture of SLP cell Li/LPSCl/NMC811 with 0.3% PTFE in the cathode, areal capacity 0.78 mAh/cm^2; (b) Electrochemical performance of the SLP, 1st cycle. The cell was tested at 60°C at the current density of 0.1 C. (1 C = 160 mAh/g) between the voltage range of 2.5 to 4.3 V.*

It should be noted, for this cell, we prepared the free-standing and flexible solid-state electrolyte consisting of 99.6% LPSCl and 0.4 wt.% PTFE. The free-standing cathode consisted of 69.7% of 1.5 nm Al_2O_3-coated NMC811, 28% LPSCl, 2% CNT, and 0.3% PTFE. The cathode has an areal-mass loading similar to that of previous disk-pouch cell, ~ 7 mg/cm^2, corresponding to areal capacity of 0.78 mAh/cm^2.

Fig. 55 showed the SLP cell performance with 0.4% PTFE in SSE, and 0.3% PTFE in s-NMC811cathode, respectively. The specific capacity of NMC811 at first cycle is 193 mAh/g with a very low coulombic efficiency of 60.3%. However, the specific capacity of NMC811 increased to 220 mAh/g at the second cycle, and the CE increased to 90%, indicating that certain cycles at the beginning are in the "cell formation" stage. The CE increased to 94.5% for the third cycle. The CE remains almost consistent after 7 cycles, with a value of 99.5%, indicating the long-term cycle life of the SSB.

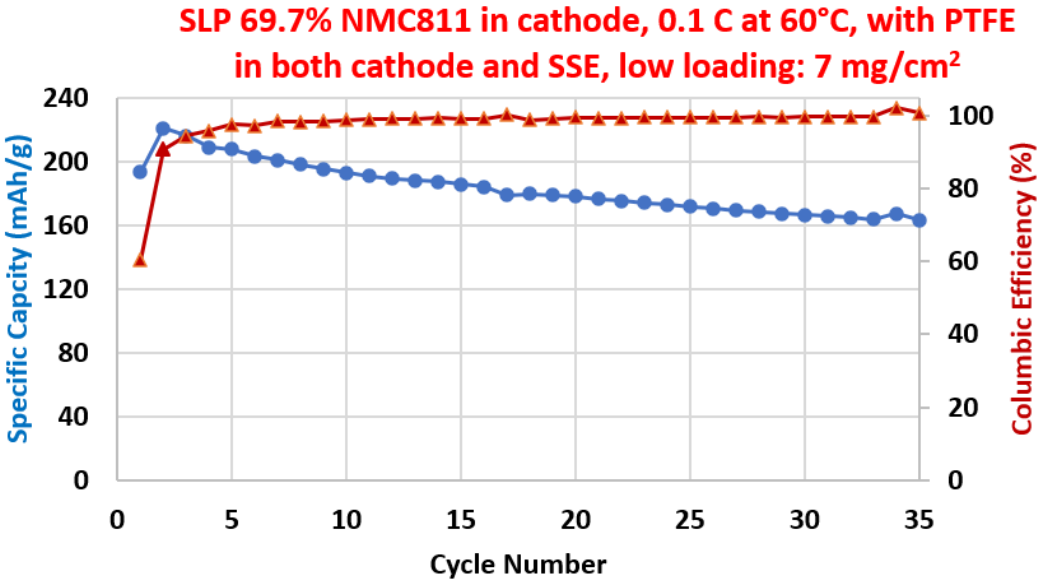

Figure 55. Specific capacity (•) and coulombic efficiency (Δ) of SLP cell Li/LPSCl/NMC811 with 0.3% PTFE in the cathode, areal capacity 0.78 mAh/cm^2.

48. *Evaluate the DLP cells with Free-Standing 1.5 nm-Al_2O_3 coated NMC811 cathode film with low percentage of PTFE binder*

Figure 56 showed the performance of DLP (Cell-stack was pressed under 6 tons), the specific capacity of NMC811 is very low, only ~ 30 mAh/g, much lower than that of single-layer pouch cell. It must be noted that the loading of active materials in the DLP is very high, ~ 24.9 mg/cm^2.

The low specific capacity can be also reflected from the low coulombic efficiency. The difference in the specific capacity of NMC811 between SLP and DLP is probably due to the difference in loading of active materials, interface resistance, thickness of SSE, and different batches of SSE. It was also noticed that DLP needs to be tested under much higher pressure to make sure the multiple interfaces are tightly contacting each other.

On the other hand, the Li metal anode was not protected in the DLP, the high charge-discharge current may accelerate the side reactions between Li anode and SSE, SSE and active carbon, SSE and NMC811, respectively.

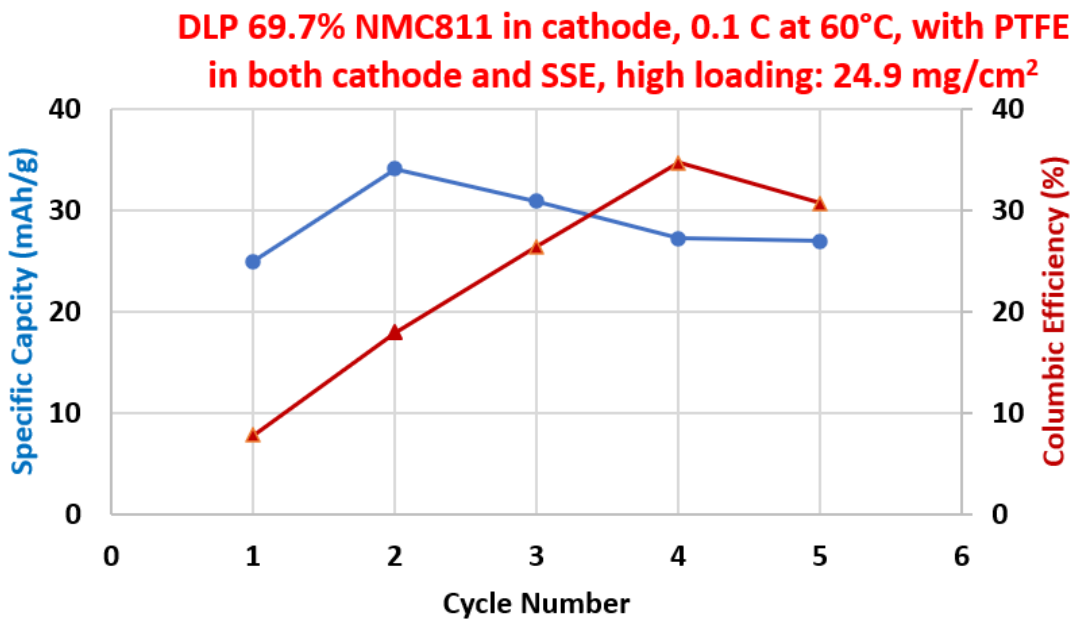

Figure 56. Specific capacity (•) and coulombic efficiency (Δ) of DLP cell Li/LPSCl/NMC811 with 0.3% PTFE in the cathode, areal capacity 2.77 mAh/cm².

The cell performance of SLP and DLP is affected by so many factors as mentioned above. Definitely, mass loading of the active materials is one of the most important factors. We are working on the reproducibility of both SLP and DLP.

Project Summary

In Phase I:

- Navitas has fully met Milestones 1.1 (SSE stable in dry room for 30 minutes).
  - Completed
- Navitas has fully met Milestones 1.2 (SSE ionic conductivity $\geq 10^{-4}$ S/cm).
  - Completed
- Navitas has fully met Milestones 2.1 (Film area ≥ 10 cm^2; SSE layer $\leq$ 100μm).
  - Completed
- Navitas has fully met Milestones 3.1 (Initial anode protection).
  - Completed
- Navitas has fully met Milestones 4.1 (Initial solid-state cell assembled).
  - Completed
- Navitas has fully met Milestones 6.1 (SSE stable in dry room for 2 h).
  - Completed

In Phase II:

Navitas has fully met Milestones 1.1 (Air stability 4 hours Li ion conductivity 0.5×10^{-3} S/cm).
  - Completed, Q2 FY2020
- Navitas has fully met Milestones 1.2 (The air stability of one doped LPS SSE (~0.5 mS/cm) has been tested and can roughly reach to 8 hours, 77% ionic conductivity retention after 8-hour exposing to dry air).

  - Completed, Q3 FY2020
- Navitas has fully met Milestones 3.1 (Li anode with thickness ≤ 50 μm fabricated, ORNL).
  - Completed, Q4 FY2020
- Navitas has fully met Milestones 3.2 (Protective layer process down-selected, UMD has proved a LiF-rich SEI on Li surface by wet chemistry).
  - Completed, Q4 FY2020
- Navitas has fully met Milestones 4.1 (Developing cathode for solid-state battery with loading ≥ 3 mAh/cm^2).
  - Completed, Q1 FY 2020
- Navitas has fully met Milestones 5.3 (12 preliminary cells assembled and shipped to DOE).
  - Completed, Q3 FY2020
- Navitas has fully met Milestones 2.2 (Demonstrate 500g cathode powder production).
  - Completed, Q4, FY 2020

In Phase II: NO-COST EXTENSION:

- Navitas has partially met Milestones M6.1 (500 Wh/kg cell demonstration).
  - In progress, we demonstrate SLP with free-standing cathode, SSE films with a potential energy density of 500 Wh/kg)
- Navitas has partially met Milestones M6.2 (Cycle life of 1000 cycles).
  - In progress, SLP with free-standing cathode, SSE films is cycling toward 50 cycles.

SECTION II. ISSUES, RISKS, AND MITIGATION:

To scale-up the Dry-Process of cathode composite, a dry-room/argon protection is needed for safety concern.

SECTION III. CHANGES IN APPROACH:

No changes in approach

SECTION IV. KEY PERSONNEL:

No changes in key personnel or teaming arrangements.

SECTION V. PROJECT OUTPUT:

A. Publications	1
B. Technologies/Techniques:	N/A
C. Status Reports:	Phase I/II/NCE quarterly report, Final reports.
D. Media Reports:	N/A
E. Invention Disclosures:	N/A
F. Patent Applications:	1
G. Licensed Technologies:	N/A
H. Networks/Collaborations Fostered:	N/A
I. Websites Featuring Project Work or Results:	N/A
J. Other Products:	N/A
K. Awards, Prizes, and Recognition:	Battery 500 Consortium FY20 Q1 Review Meeting, Poster Presentation, Best Poster Award

SECTION VI. FOLLOW-ON FUNDING: N/A

SECTION VII. RECIPIENT AND PRINCIPAL INVESTIGATOR DISCLOSURES: N/A

SECTION VIII. CONFLICTS OF INTERESTS WITHIN PROJECT TEAM: N/A

SECTION IX. PERFORMANCE OF WORK IN THE UNITED STATES:

All work is being performed in the United States.

SECTION X. PROJECT SCHEDULE STATUS for Phase I/II:

MS# Phase I	Milestone Description	Milestone Type	Ant. Qtr.	Start date	Status (Completion %)
M1.1	SSE stable in dry room for 30 minutes	Technical	Q2	Feb. 2018	100% completion
M1.2	SSE ionic conductivity $\geq 10^{-4}$ S/cm	Technical	Q3	Feb. 2018	100%
M2.1	Film area ≥ 10 cm^2; SSE layer $\leq$ 100µm	Technical	Q4	Feb. 2018	100%
M3.1	Low impedance anode mate to cathode/SSE bilayer	Technical	Q3	Feb. 2018	100%
M4.1	Initial solid-state cell assembled	Technical	Q4	April 2018	100%
M5.1	Down select process parameters	Technical	Q5	Dec. 2017;	100%
M5.2	Cathode loading $\geq$ 3.0 mAh/cm^2	Technical	Q6	April 2018	100%
M6.1	SSE stable in dry room for 2 h	Technical	Q6	April 2018	100%
M6.2	SSE stable 0 – 5 V	Technical	Q6	April 2018	70%
M7.1	Film area ≥ 30 cm^2; SSE layer thickness $\leq$50 µm	Technical	Q6	July 2018	60%
M8.1	Laminable protected Li anode	Technical	Q6	July 2018	50%
M9.1	Solid state cell assembled (TRL 4)	Technical	Q6	Oct. 2018	20%
M9.2	Feasibility for a 400 Wh/kg cell	Go / No Go	Q6	Mar. 2019	50%
M9.3	Cycle life of $\geq$ 250 (500 preferred)	Go / No Go	Q6	Mar. 2019	40%

Milestone for Phase II and NCE	Start Date		Completion date		Status (Completion %)
	Planned	Actual	Planned	Actual	
Task 1. SSE powder development					
SSE powder 4h air stability and 0.5 mS/cm	Q3, FY2019	Q3, FY2019	Q1, FY2021	Q3, FY2019;	100%
SSE powder 8h air stability and 1 mS/cm	Q3, FY2019	Q3, FY2019	Q3, FY2020	Q3, FY 2020	100%
Task 2. Cathode development					
Process down selection	Q3, FY2019	Q4, FY2019	Q1, FY2021	Q1 FY2022	90%
Demonstrate 500 g cathode powder production	Q3, FY2019	Q4, FY2019	Q1, FY2021	Q4, FY 2020	100%
Task 3. Li anode development					
Li anode thickness ≤50 µm	Q3, FY2019	Q1, FY2020	Q4 FY2021	Q4 FY2020	100%
Li anode protection method verification	Q3, FY2019	Q3, FY2020	Q4 FY2020	Q4 FY2020	100%, protection didn't work well from ORNL, UMD
Task 4. Cell stack development					
Cathode loading ≥ 3 mAh/cm^2	Q3, FY2019	Q3, FY2020	Q1 FY2022	Q1 FY2020	Completed in disk-type cell (100%)
SSE Film thickness ≤ 25 µm	Q3, FY2019	Q2, FY2020	Q1 FY2021	Q1 FY2022	In progress. 50 µm thick SSE is achieved
SLP DLP with free-standing cathode film	Q3, FY2019	Q1, FY2021	Q4 FY2021	Q1 FY2022	100%
Task 5. Cell Assembly					
12 preliminary cell delivery	Q3, FY2019	Q1, FY2020	Q2 FY2020	Q3 FY2020	100% Disk-cell in pouch.
2.5 Ah pouch cell assembly	Q3, FY2019		Q4 FY2021	n/a	Challenging due to scale-up
12 final test cell delivery	Q3, FY2019		Q4 FY2021	n/a	Challenging due to scale-up
Task 6. Cell Test					
Cell specific energy of 500 Wh/kg	Q4, FY2019	Q1 FY2020	Q4 FY2021	NCE Q1 FY2022	In progress
Cell cycle life of 1000	Q3, FY2021	Q3 FY2021	Q4 FY2021	NCE Q1 FY2022	in progress
Final Report	Q1 FY2022	Q1 FY2022	Q1 FY2022	Q1 FY2022	100%

Presentations:

- Presentation at Battery500 Seedling Projects Review Meeting, Berkeley, CA, Feb. 6, 2018
- Presentation at Battery500 Seedling Projects Review Meeting, Berkeley, CA, Aug. 1, 2018
- X Fan, X Ji, F Han, J Yue, J Chen, L Chen, T Deng, J Jiang, C Wang. *Science advances* **4** (12), eaau9245
- Battery 500 Consortium FY20 Q1 Review Meeting, Poster Presentation (Best Poster Award), San Francisco, CA, Feb. **2020**. Solvent-free and Non-sintered 500 Wh/kg All Solid-State Battery. *Robert Sosik, Sufu Liu, Mahdi Soueid, John Hopkins, James Seong, Chunsheng Wang, David Wood, Jianlin Li, Mike Wixom, James Dong, Binsong Li.*

- Battery 2020 Congress, Invited Presentation, Troy, MI, September **2020**. *Advanced Electrode Coating Technology for Li-ion Batteries.* Binsong Li.

Patent:

Compositions and Methods for Electrode Fabrication. *Binsong Li, Robert Sosik, Michael Wixom. US Patent Application #* 62/984,144. March, **2020**.